

UNCLASSIFIED

433542

AD

DEFENSE DOCUMENTATION CENTER

FOR

SCIENTIFIC AND TECHNICAL INFORMATION

CAMERON STATION, ALEXANDRIA, VIRGINIA



UNCLASSIFIED

NOTICE: When government or other drawings, specifications or other data are used for any purpose other than in connection with a definitely related government procurement operation, the U. S. Government thereby incurs no responsibility, nor any obligation whatsoever; and the fact that the Government may have formulated, furnished, or in any way supplied the said drawings, specifications, or other data is not to be regarded by implication or otherwise as in any manner licensing the holder or any other person or corporation, or conveying any rights or permission to manufacture, use or sell any patented invention that may in any way be related thereto.

64-11



ORA-63-13

ORA-63-13

CATALOGED BY DCC
AS AD No. 433542

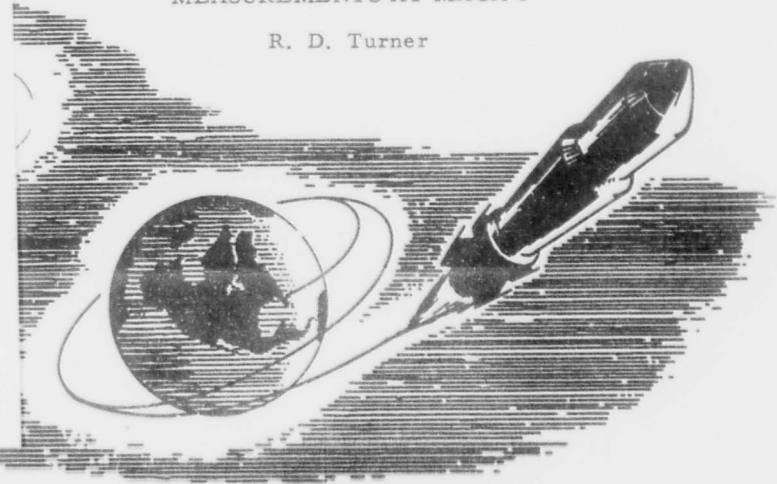
HEADQUARTERS OFFICE OF AEROSPACE RESEARCH TECHNICAL REPORT

Contract No. AF 29(600)-1711
Project No. 7856
Task No. 78548

DYNAMICS OF SEPARATING BODIES
Volume III
MEASUREMENTS AT MACH 8

R. D. Turner

433542



**OFFICE OF RESEARCH ANALYSES
HOLLOMAN AIR FORCE BASE
NEW MEXICO**

November 1963

AVAILABILITY NOTICE

Qualified requesters may obtain copies of this report from DDC. Orders will be expedited if placed through your librarian or other staff member designated to request and receive documents from DDC.

ORA-63-13

ORA-63-13

Contract No. AF 29(600)-1711
Project No. 7856
Task No. 78548

DYNAMICS OF SEPARATING BODIES

Volume III

MEASUREMENTS AT MACH 8

by

R. D. Turner
Cook Research Laboratories
A Division of
Cook Electric Company
Chicago, Illinois

Science and Engineering Analyses Division
Office of Research Analyses

OFFICE OF AEROSPACE RESEARCH
UNITED STATES AIR FORCE
Holloman Air Force Base, New Mexico

November 1963

FOREWORD

This report was prepared under Air Force Contract No. AF 29(600)-1711, Project No. 7856, Task No. 78548, by the Tech-Center Division, Cook Electric Company, Morton Grove, Illinois. This contract was monitored by the Air Force Office of Scientific Research. The technical advisor was Mr. F. Utech, Aerospace Engineer for Flight Systems, Office of Research Analyses, Holloman AFB, New Mexico.

The work was performed under the general direction of Mr. Alton D. Anderson, Vice President of the parent company and General Manager of the Tech-Center Division and Mr. R. C. Edwards, Vice President of the parent company and Director of Cook Research Laboratories.

The technical effort was carried out by the Aerospace Technology Section under the direction of Mr. L. J. Lorenz, Section Manager and Dr. R. J. Benjamin, Director of Engineering. Mr. L. W. Sims was Program Manager and Mr. R. Turner conducted the tests performed at Tunnel B.

Other members of the staff who significantly assisted with the project were Messrs. J. Buday, F. Doerr, B. Hedien, H. Karp, P. Minerva, O. Ostrem, A. Solarski, H. Wackelin and R. Wolter.

The wind tunnel tests were conducted in Wind Tunnels E-2 and B of the von Karman Gas Dynamics Facility, Arnold Engineering Development Center. The cooperation and effort afforded this program by the Air Force and ARO personnel concerned was especially valuable.

ABSTRACT

Additional wind tunnel tests at a Mach number of 8, which supplement Mach 2, 4 and 5 tests reported in Volume II on a data capsule shape in an interference flow field of a carrier vehicle were conducted. The data obtained were analyzed and a preliminary evaluation was made as to the agreement with methods of prediction for both the Mach 8 tests and previous reported tests. It is shown that where the interference flow field is reasonably predicted, estimated values of a capsule's derivatives obtained with relatively simple calculation techniques agree reasonably well with the data.

KEYWORDS

Dynamics of Separation
Wind Tunnel Tests, Supersonic
Ejection - Capsules

TABLE OF CONTENTS

<u>Section</u>	<u>Page</u>
I. INTRODUCTION	1
II. WIND TUNNEL TESTS	2
A. AEDC Wind Tunnels E-2 and B	3
B. Models and Equipment	3
C. Test Procedure	5
III. SUMMARY OF DATA	10
IV. DATA ANALYSIS	33
A. Close-in Effects	33
B. Wake Penetration	36
C. Wake-Capsule Interaction	37
V. CONCLUSIONS	48

LIST OF ILLUSTRATIONS

<u>Figure No.</u>		<u>Page</u>
1	Dimensions of Models Employed in Proximity Tests . . .	6
2	Capsule Sting Assembly Used in Tunnel B Tests	7
3	Coordinate System and Test Positions Surveyed	8
4	Wake Penetration Coordinate System	9
5	Free Stream Capsule Characteristics - Variation of Axial Force, Normal Force and Pitching Moment Coefficients with Angle of Attack	11
6a	Close-in Data - Variation of Capsule Characteristics with Axial Excursion in Carrier Flow Field - Lateral Station $Y_c/D = 0.75$	12
6b	Close-in Data - Variation of Capsule Characteristics with Axial Excursion in Carrier Flow Field - Lateral Station $Y_c/D = 0.875$	13
6c	Close-in Data - Variation and Capsule Characteristics with Axial Excursion in Carrier Flow Field - Lateral Station $Y_c/D = 1.0$	14
6d	Close-in Data - Variation of Capsule Characteristics with Axial Excursion in Carrier Flow Field - Lateral Station $Y_c/D = 1.125$	15
6e	Close-in Data - Variation of Capsule Characteristics with Axial Excursion in Carrier Flow Field - Lateral Station $Y_c/D = 1.25$	16
6f	Close-in Data - Variation of Capsule Characteristics with Axial Excursion in Carrier Flow Field - Lateral Station $Y_c/D = 1.375$	17
6g	Close-in Data - Variation of Capsule Characteristics with Axial Excursion in Carrier Flow Field - Lateral Station $Y_c/D = 1.50$	18

LIST OF ILLUSTRATIONS (cont'd.)

<u>Figure No.</u>		<u>Page</u>
6h	Close-in Data - Variation of Capsule Characteristics with Axial Excursion in Carrier Flow Field - Lateral Station $Y_C/D = 1.625$	19
6i	Close-in Data - Variation of Capsule Characteristics with Axial Excursion in Carrier Flow Field - Lateral Station $Y_C/D = 1.75$	20
6j	Close-in Data - Variation of Capsule Characteristics with Axial Excursion in Carrier Flow Field - Lateral Station $Y_C/D = 2.00$	21
6k	Close-in Data - Variation of Capsule Characteristics with Angle of Attack at Specified Values of Y_C/D , Axial Station $X_C/D = 0$	22
6l	Close-in Data - Variation of Capsule Characteristics with Angle of Attack at Specified Values of Y_C/D , Axial Station $X_C/D = 0.5$	23
6m	Close-in Data - Variation of Capsule Characteristics with Angle of Attack at Specified Values of Y_C/D , Axial Station $X_C/D = 0.75$	24
6n	Close-in Data - Variation of Capsule Characteristics with Angle of Attack at Specified Values of Y_C/D , Axial Station $X_C/D = 2.25$	25
6o	Close-in Data - Variation of Capsule Characteristics with Angle of Attack at Specified Values of Y_C/D , Axial Station $X_C/D = 3.5$	26
7a	Close-in Phase - Shadowgraph Sequence Showing Axial Travel of Capsule at Lateral Separation $Y_C/D = 0.75$, $\alpha = 0$	27
7b	Close-in Phase - Shadowgraph Sequence Showing Axial Travel of Capsule at Lateral Separation $Y_C/D = 1.00$, $\alpha = 0$	28

LIST OF ILLUSTRATIONS (cont'd.)

<u>Figure No.</u>		<u>Page</u>
8a	Capsule Penetration of the Wake Boundary	29
8b	Capsule Penetration of the Wake Boundary	30
9a	Variation of Axial Force Coefficient Along the Carrier Wake Axis for a Free Stream $Re = 3.36 \times 10^6/Ft$. . .	31
9b	Variation of Axial Force Coefficient Along the Carrier Wake Axis for a Free Stream $Re = 1.69 \times 10^6/Ft$. . .	32
10	Comparison of Measured Shock Wave Location and Angle with Values Obtained from Characteristic Solution for a 15 Degree Half Angle Cone, Cylinder Body Combination	40
11a	Predicted Close-in Aerodynamic Coefficients - Variation of Capsule Characteristics with Axial Excursion in a Flow Field Generated by the Method of Characteristics of a 15 Degree Half Angle Cone Cylinder, Lateral Station $Y_c/D = 0.75$	41
11b	Predicted Close-in Aerodynamic Coefficients - Variation of Capsule Characteristics with Axial Excursion in a Flow Field Generated by the Method of Characteristics for a 15 Degree Half Angle Cone Cylinder Lateral Station $Y_c/D = 1.00$	42
11c	Predicted Close-in Aerodynamic Coefficients - Variation of Capsule Characteristics with Axial Excursion in a Flow Field Generated by the Method of Characteristics for a 15 Degree Half Angle Cone Cylinder Lateral Station $Y_c/D = 1.25$	43
11d	Predicted Close-in Aerodynamic Coefficients - Variation of Capsule Characteristics with Axial Excursion in a Flow Field Generated by the Method of Characteristics for a 15 Degree Half Angle Cone Cylinder Lateral Station $Y_c/D = 1.50$	44

LIST OF ILLUSTRATIONS (cont'd.)

<u>Figure No.</u>		<u>Page</u>
12	Capsule Axial Force Coefficient Variation with Free Stream Mach number and Various Reynolds Numbers . .	45
13a	Comparison of Predicted and Experimental Data for Wake Core Drag Ratio - $Re = 3.36 \times 10^6$ Ft.	46
13b	Comparison of Predicted and Experimental Data for Wake Core Drag Ratio - $Re = 1.69 \times 10^6$ Ft.	47

LIST OF SYMBOLS

A	Axial force
A_B	Capsule base area
C_A	Axial force coefficient $A/q_\infty A_B$
C_{AT}	Total axial force coefficient
C_M	Pitching moment coefficient $M/q_\infty A_B L$
C_N	Normal force coefficient $N/q_\infty A_B$
D	Carrier vehicle body diameter
Dw	Drag force on capsule in wake
D_∞	Drag force on capsule in free stream
L	Capsule length
M	Pitching moment about capsule center of gravity or free stream Mach number
N	Normal force
Po	Wind tunnel stilling chamber pressure
q	Dynamic pressure
Re	Reynolds number
X	Streamwise direction, measurement or position coordinate
Y	Direction measurement or position coordinate in pitch plane, transverse to the stream direction
α	Angle of attack of capsule model centerline to the free stream direction
c	Subscript used when the coordinates are those of the capsule
∞	Subscript refers to free stream tunnel conditions
θ	Shock wave angle referenced to the carrier vehicle centerline (degrees)

SECTION I

INTRODUCTION

This report presents a summary of wind tunnel tests conducted at a Mach number of 8 and the evaluation of data therefrom. These tests were performed as a part of a second phase of work which consisted of these data and data previously obtained at Mach numbers of 2, 4, and 5 which are reported on in Volume II (Ref. 1). The first phase of this contract on Dynamics of Separation has been reported in Volume I and consists of the results of a study program where analytical techniques were developed for the purpose of determining the behavior of capsule bodies separating from high performance vehicles.

The wind tunnel tests reported on herein were conducted to provide static force measurements on a capsule at various positions within an interference flow field. These measurements provide a basis for which analytical techniques, which may be used in predicting the interference flow field effects, can be evaluated. These tests were conducted in the AEDC wind tunnel B at a Mach number of 8.1. The models used for these tests, and the lower Mach number tests reported in Volume I, consisted of a flared body capsule and a carrier vehicle model representative of a high performance rocket vehicle. These models are discussed in Section II along with the test procedures followed. The capsule data obtained are presented in Section III and a series of Shadowgraph photographs of a run sequence are also shown. A preliminary evaluation of the static data and the correlation with predicted values are presented in Section IV and the application of the data to the development of empirical-theoretical procedures is considered.

SECTION II

WIND TUNNEL TESTS

Two wind tunnel tests were conducted to enable the acquisition of static data at a Mach number of 8 for the Cook Research Laboratories' capsule model. The first test program was performed in the E-2 Tunnel at AEDC between 16 May and 24 May 1960. This test program was performed to determine the adequacy of the water cooling system incorporated in the same size capsule model used in the tests at Mach numbers of 2, 4, and 5.

The test program was comprised of two separate tests. The first test incorporated a thermobalance in the capsule which allowed measurements of the balance beam temperatures for various water flow rates and wind tunnel total pressures and temperatures. The second series of tests incorporated the CRL capsule model balance installed in the model and bridge output data were recorded through an angle of attack range and various water flow rates and wind tunnel conditions. The thermobalance tests were performed at a Mach number of 7 and stagnation temperatures up to 700°F. The stagnation pressure, however, was raised to a point where the heat input was greater than for Tunnel B operating conditions at Mach 8.0. The bridge output balance tests were conducted at Mach numbers of 7 and 8 and stagnation temperatures up to 900°F. The results of these tests indicated that no significant variation in balance temperatures is encountered with angle of attack, water pressure, or tunnel stagnation pressure (heat input) and that the balance operation is satisfactory under these conditions.

As a result of this verification of the water cooling design for the capsule model, the proximity tests were conducted in Tunnel B between 30 June to 28 July 1962. These tests measured the capsule static coefficients while in the interference flow field surround the side, and base region of the carrier model. Close-in data were obtained by positioning the capsule model laterally and axially in the side flow field of the carrier model; wake-penetration data were obtained by traversing the capsule model across the wake boundary behind the carrier base; and wake-capsule interaction data were obtained by traversing the capsule axially down the wake centerline.

A. AEDC Wind Tunnels E-2 and B

The AEDC Tunnel E-2 is a 12 x 12 inch intermittent hypersonic wind tunnel with a Mach number range of 4.5 to 8.0. An upstream high pressure air storage system and a vacuum sphere downstream provide the necessary pressure ratio across the wind tunnel. Electric heaters upstream of the stilling section provide air temperatures up to 900°F to prevent liquefaction of the main stream. The test section is equipped with a vertical sector which provides an angle of attack range of ± 11 degrees with a straight sting. A shadowgraph system is available for photo observation of flow fields.

The 50 inch Mach 8 Tunnel B is an axisymmetric, continuous flow, variable density, hypersonic wind tunnel with a 50 inch diameter test section. Because of changes in boundary-layer thickness caused by changing pressure level, the Mach 8 contoured nozzle produces an average test section Mach number which varies from 8.0 at a stagnation pressure of 100 psia to 8.1 at 900 psia. Stagnation pressure up to approximately 900 psia is supplied to the tunnel by the VKF 92, 500-hp compressor system. The air is selectively valved through the compressor system, high pressure driers, and the propane fired heater. The heater produces a maximum air temperature of 900°F, sufficient to prevent liquefaction of the air in the test section.

B. Models and Equipment

The capsule model balance, capsule and carrier vehicle models, stings, and the auxiliary positioning equipments used in these tests, with the exception of the ARO axial actuator, were designed and manufactured by the Cook Research Laboratories for the tests previously conducted in Tunnel A, and modified for Tunnel B operation, as part of the contract. Figure 1 shows the general dimension of the capsule and carrier vehicles models used in the proximity tests.

The capsule model used in this program was a modified version of the capsule used in the Mach 2, 4, and 5 tests and incorporated a water cooling system that was adequate to prevent the model balance from being overheated during tunnel operating conditions. This modification could not be performed by the standard procedure of putting a water jacket around the model balance since the internal space within the capsule model would not accommodate this type of installation. As a result of the space restriction, primarily in the cylindrical portion of the capsule, an alternate approach of incorporating effectively two water tanks, one in the nose and one in the flare, was used. These tanks were connected in parallel to the inlet source and the water flow rate was divided in a 5 to 3

ratio for front to rear tanks, respectively. Both the inlet and return water lines were routed through the model sting and incorporated flexible bellows to allow force measurements to be taken. Figure 2 shows the capsule and sting assembly.

The ASP, auxiliary sting positioner, which was used to position the capsule laterally and provide an angle of attack range of $\pm 20^\circ$ for the close-in phase of the testing, was modified with water lines and jackets at all accessible locations; however, it could not be made to function remotely in the lateral direction without complete redesign. Sufficient cooling and design modification were incorporated in the angle of attack mechanism so that remote operation was successful, despite thermal expansion, hence during the test tunnel shutdowns were required only when manual lateral translation was required. For the close-in tests, the carrier vehicle was remotely positioned in the axial direction by the ARO axial actuator and thereby allowed the acquisition of data for various X_c/D locations.

The wake penetration tests were conducted by ceiling mounting a second carrier model and probing the wake with the capsule model mounted on the ASP. For the wake core tests, the same carrier model and sting assembly used in the wake penetration tests were used. In these tests, however, the capsule was traversed along the wake core at various axial locations by use of the ARO axial actuator to which the capsule and sting assembly were mounted.

The forces and moments on the capsule were measured by a miniature internal electric strain gage balance. This balance was a compound, split-type designed to measure normal force, axial force and pitching moment in a single plane.

The balance and capsule model assembly was calibrated at AEDC with cooling water flowing to account for the effect of variations in water pressure. The design calibration loads were six pounds of normal force and six pounds of axial force. As stated in Reference 2, a post calibration of the assembly indicated the axial force scale factor decreased by approximately 3 percent. As a result, the values shown may be as much as 3 percent high; other scale factors checked to within 0.5 percent, however. The other source of possible error, reported in Reference 2, is an angle of attack error of approximately 1° . This potential error results from clearances that were designed into the ASP based on estimated thermal expansion characteristics that provided play which could be measured before and after tunnel operation (reduced temperature).

C. Test Procedure

The test positions surveyed in the proximity tests are shown in Figures 3 and 4. For the side flow field and wake penetration tests, various angles of attack were obtained at each specific position shown. For these tests, the angle of attack is referenced to the carrier vehicle's centerline and is considered positive when the capsule's nose is pointing away from the carrier. For the wake core tests, the angle of attack was zero.

Data were obtained for the following conditions:

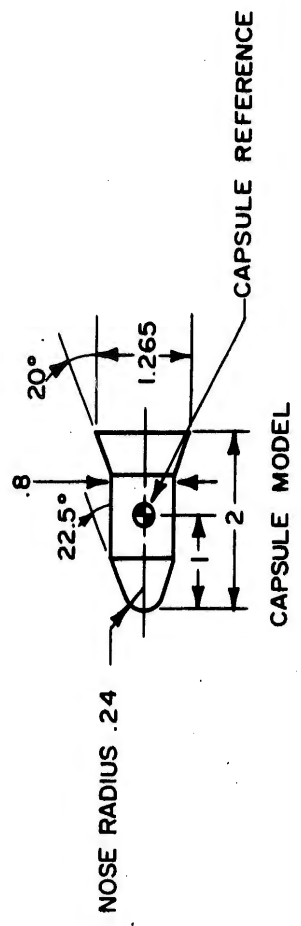
<u>Type of Test</u>	<u>Mach No.</u>	<u>P_o (psia)</u>	<u>T_o (°R)</u>	<u>Re_D</u>
Close-in Effects	8.092	800	1350	2.24 x 10 ⁵
Wake Penetration	8.092	800	1350	2.24 x 10 ⁵
Wake Capsule Inter- action (2 Tests)	8.092 8.067	800 400	1350 1350	2.24 x 10 ⁵ 1.13 x 10 ⁵

P_o = Tunnel stilling chamber pressure

T_o = Tunnel stagnation pressure

Re_D = Reynolds number based on capsule cylinder diameter

In addition to the above tests, free stream force and moment coefficients were obtained for reference purposes and data analysis. The capsule data obtained were axial force, normal force, and pitching moment coefficients. Capsule base pressure coefficient was also obtained for most of the test runs. Shadowgraph photographs were taken at various data points.



ALL LINEAR DIMENSIONS IN INCHES.

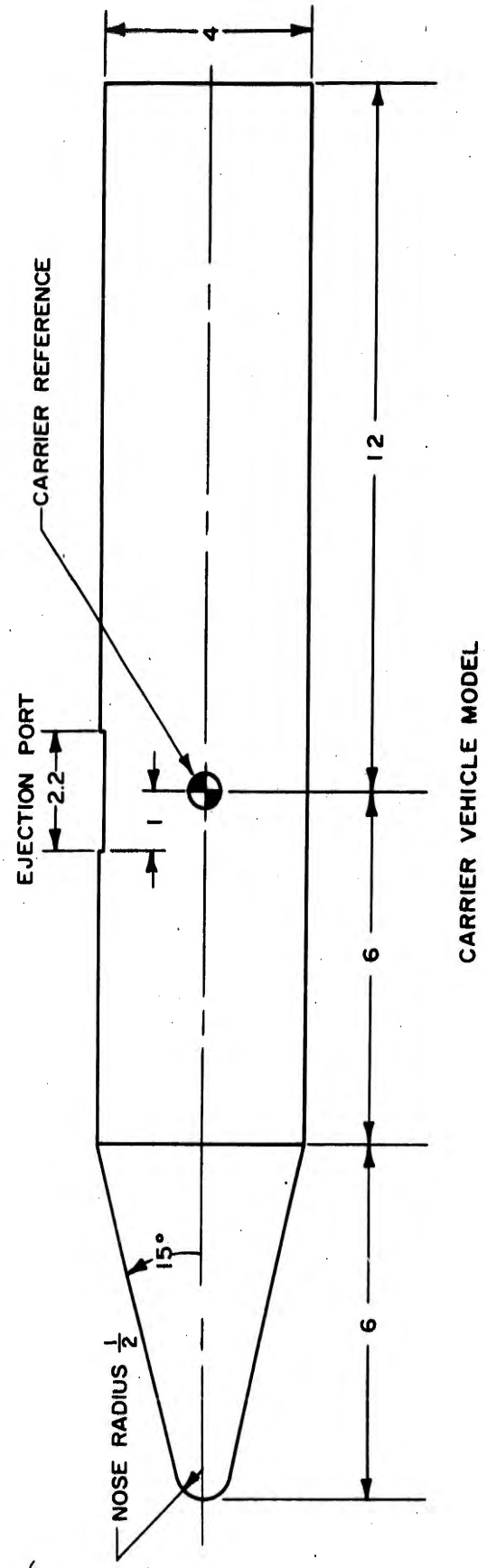


Figure 1. Dimensions of Models Employed in Proximity Tests



7

Figure 2. Capsule Sting Assembly Used in Tunnel B Tests

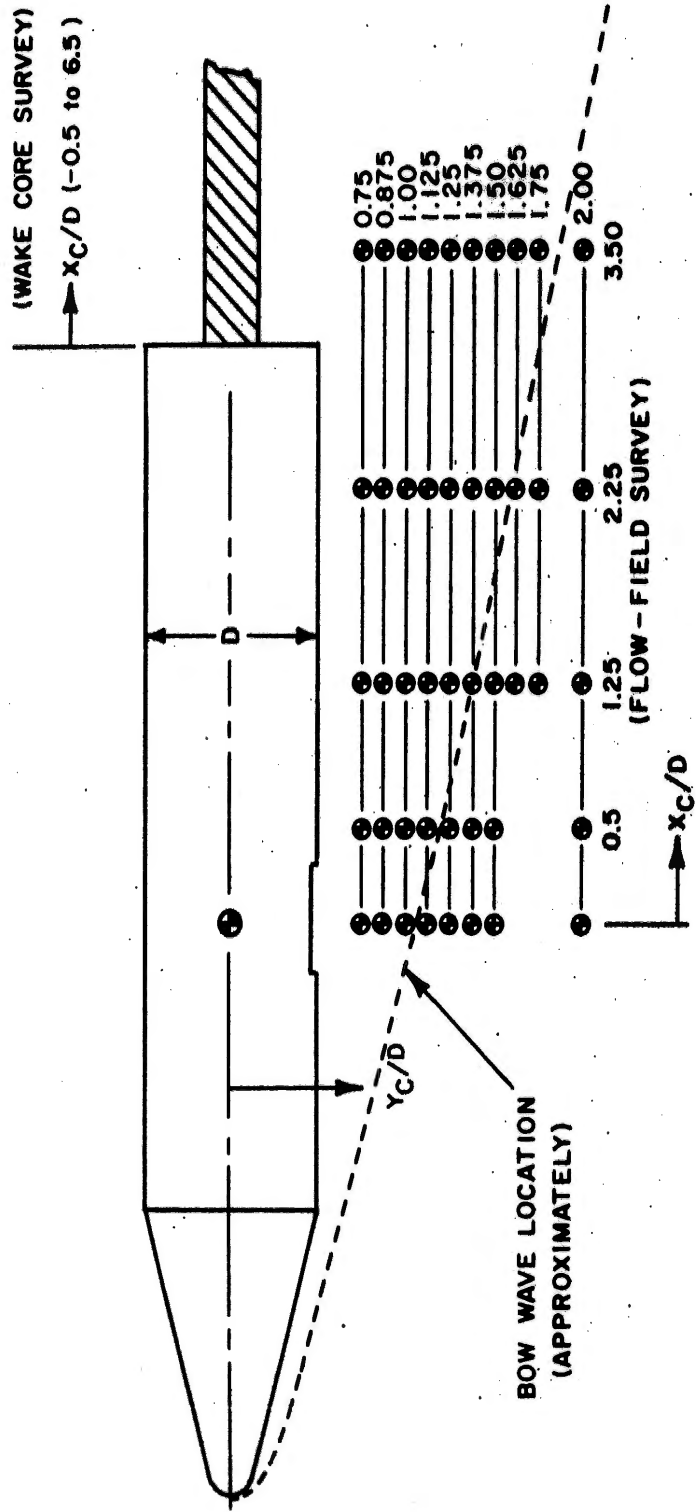


Figure 3. Coordinate System and Test Positions Surveyed

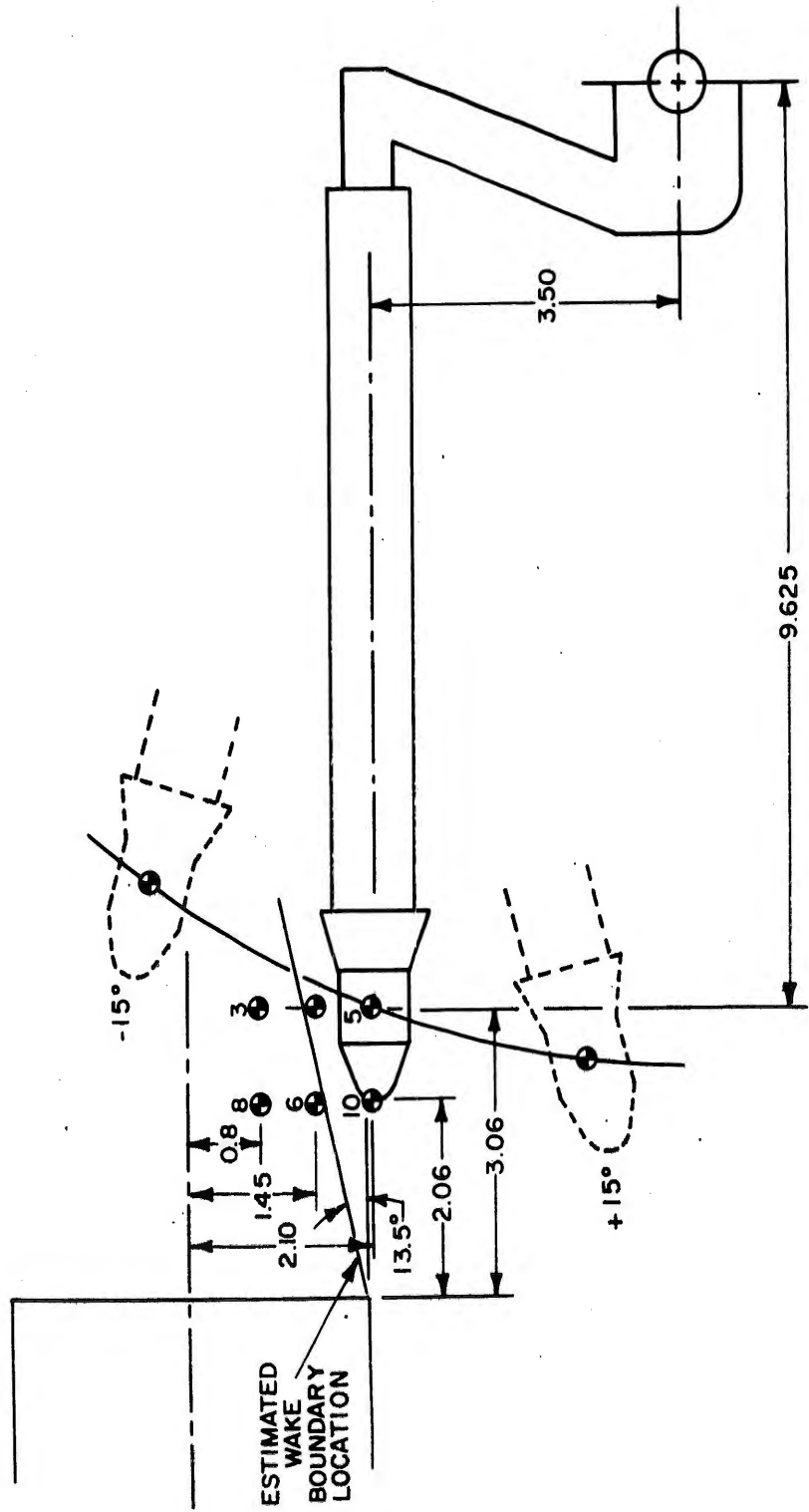


Figure 4. Wake Penetration Coordinate System

SECTION III

SUMMARY OF DATA

A summary of the test data obtained is shown in Figures 5 to 9b. These data are, for the most part, as obtained from the wind tunnel data reduction and only obvious zero shifts have been compensated for.

Figure 5 presents the capsule free stream characteristics obtained at a Reynolds number of 3.36×10^6 per foot. These data were obtained by positioning the capsule as far forward and above the carrier vehicle, thereby as far forward of the carrier bow shock, as possible. The faired curves through the data scatter have been used in comparing the interference flow field data with the free stream characteristics.

The close-in data are shown in Figures 5a to 6o. In Figures 6a to 6j, the capsule coefficients are shown for various lateral positions and axial travel. The remaining figures show the effect of lateral travel for a fixed axial location as a function of the capsule pitch angle. In these graphs, the free stream coefficients are given for comparison purposes. Shadowgraph pictures showing typical shockwave patterns for the capsule in the interference flow field and carrier bow shockwave interaction with the capsule are shown in Figures 7a and 7b.

The wake penetration data are given in Figures 8a and 8b. These data were obtained by positioning the capsule at zero pitch angle at two axial locations behind the carrier vehicle and three lateral positions at each axial location (Figure 4). From these six locations, the capsule was pitched through $\pm 15^\circ$. The resultant changes in axial (Δx) and lateral (Δy) locations from the zero pitch angle position are given by the following equations:

$$\Delta x = -10.242 \cos (\alpha - 19.98) + 9.625$$

$$\Delta y = 10.242 \sin (\alpha - 19.98) + 3.5$$

where α is in degrees and Δx and Δy are in inches.

Wake capsule interaction data were obtained at two tunnel free stream Reynolds numbers. These data were obtained for capsule axial positions referenced to the nose of the capsule and the base of the carrier vehicle of -0.5 to $+6.5$ carrier vehicle diameters. All of these measurements were obtained at zero pitch angle and the variations of C_N and C_M recorded were extremely small and are not presented. The values of C_A with axial position are shown in Figures 9a and 9b for the two tunnel Reynolds numbers.

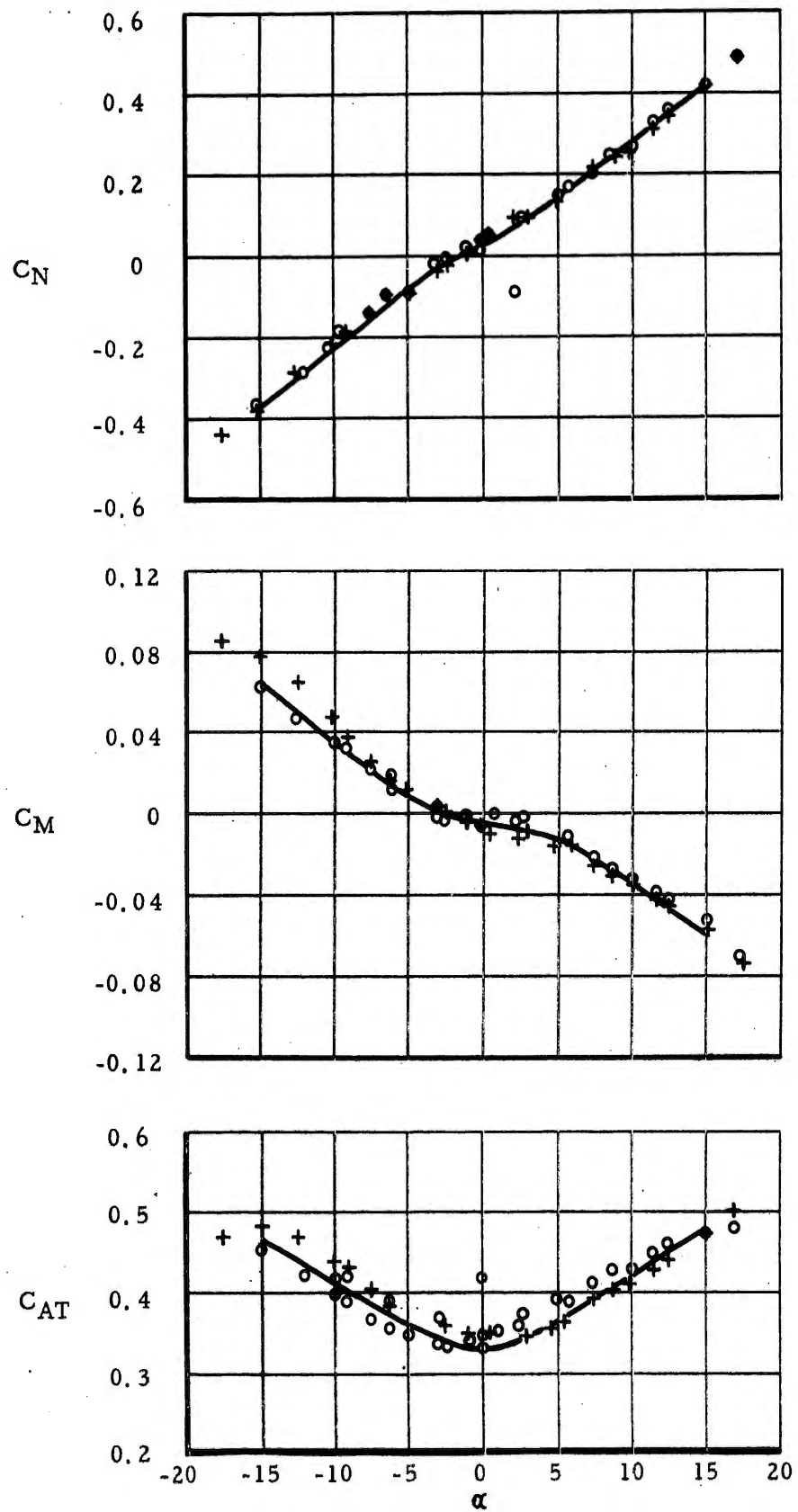


Figure 5 , Free Stream Capsule Characteristics - Variation of Axial Force, Normal Force and Pitching Moment Coefficients with Angle of Attack (Degrees)

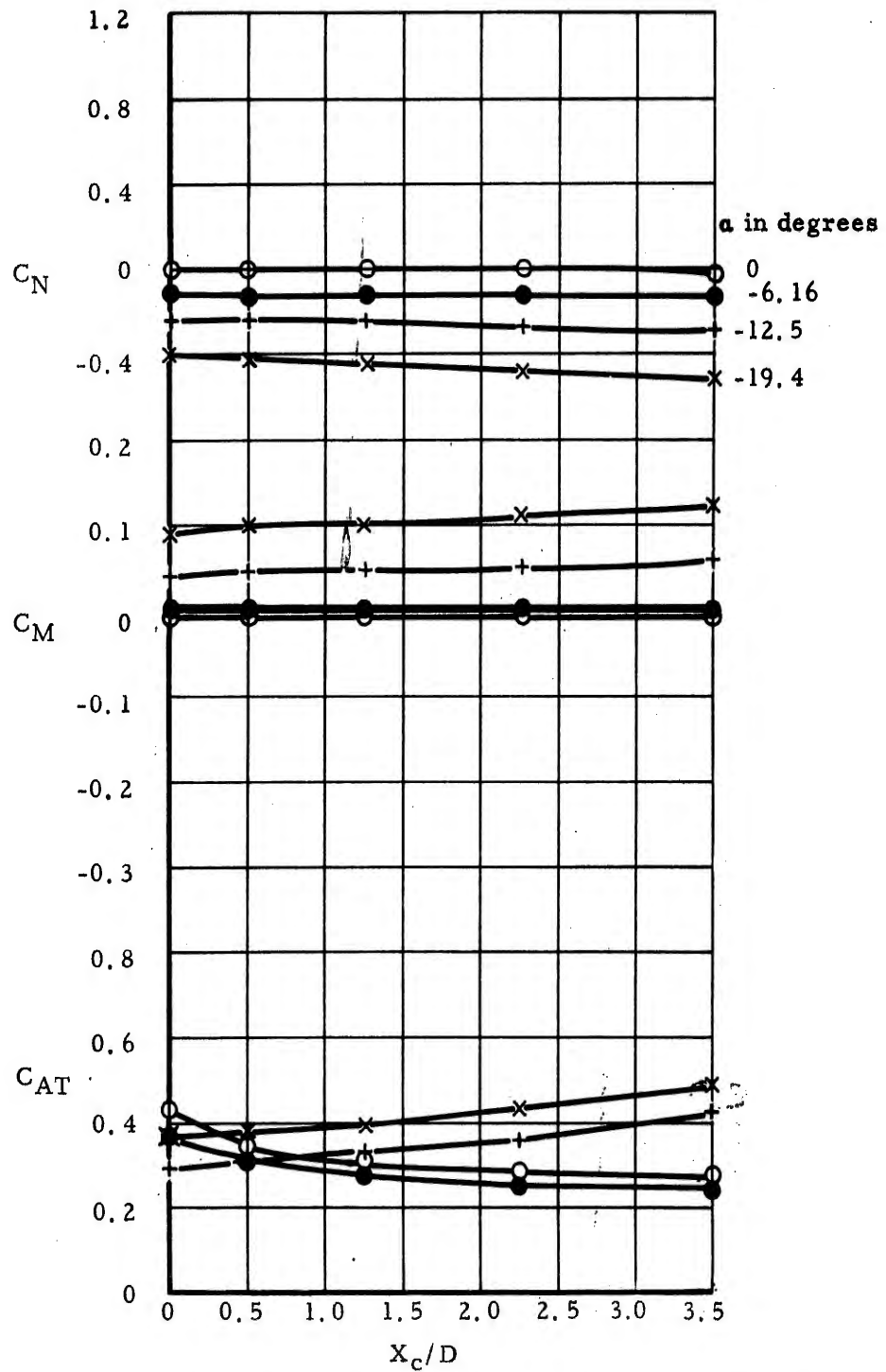


Figure 6a. Close-in Data - Variation of Capsule Characteristics with Axial Excursion in the Carrier Flow Field - Lateral Station $Y_c/D = .75$

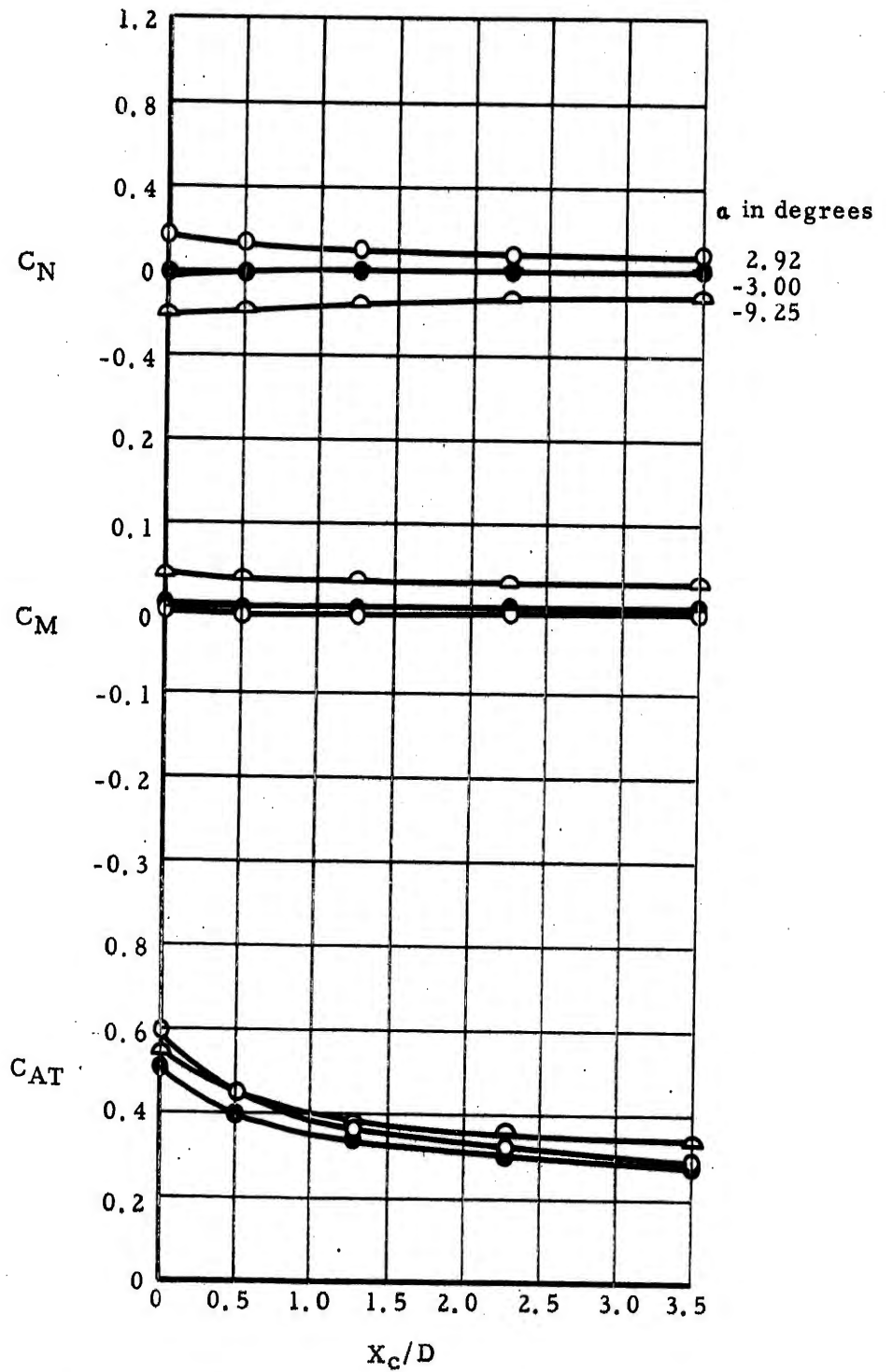


Figure 6b. Close-in Data - Variation of Capsule Characteristics with Axial Excursion in the Carrier Flow Field - Lateral Station $Y_c/D = .875$

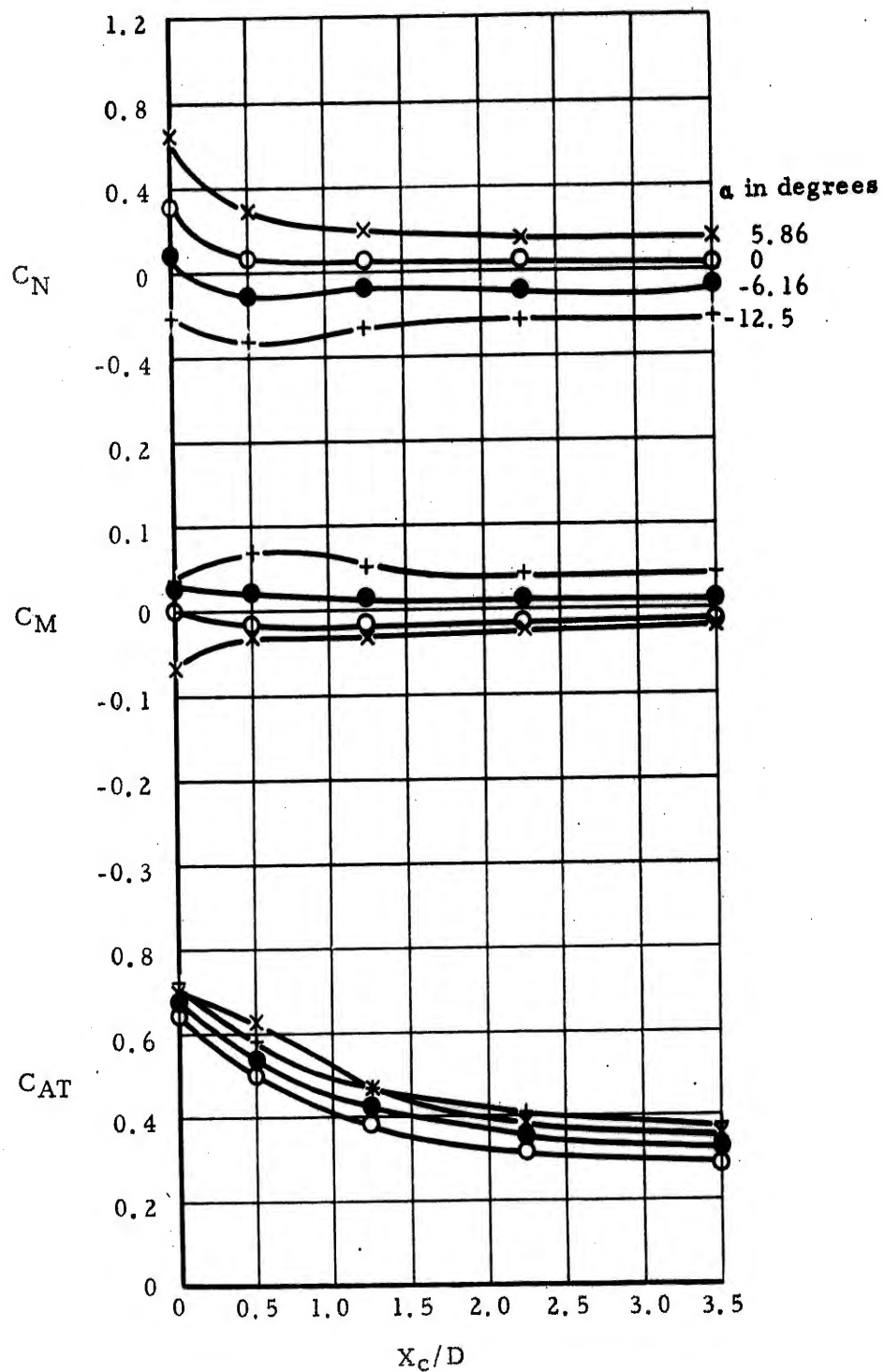


Figure 6c. Close-in Data - Variation of Capsule Characteristics with Axial Excursion in the Carrier Flow Field - Lateral Station $Y_c/D = 1.0$

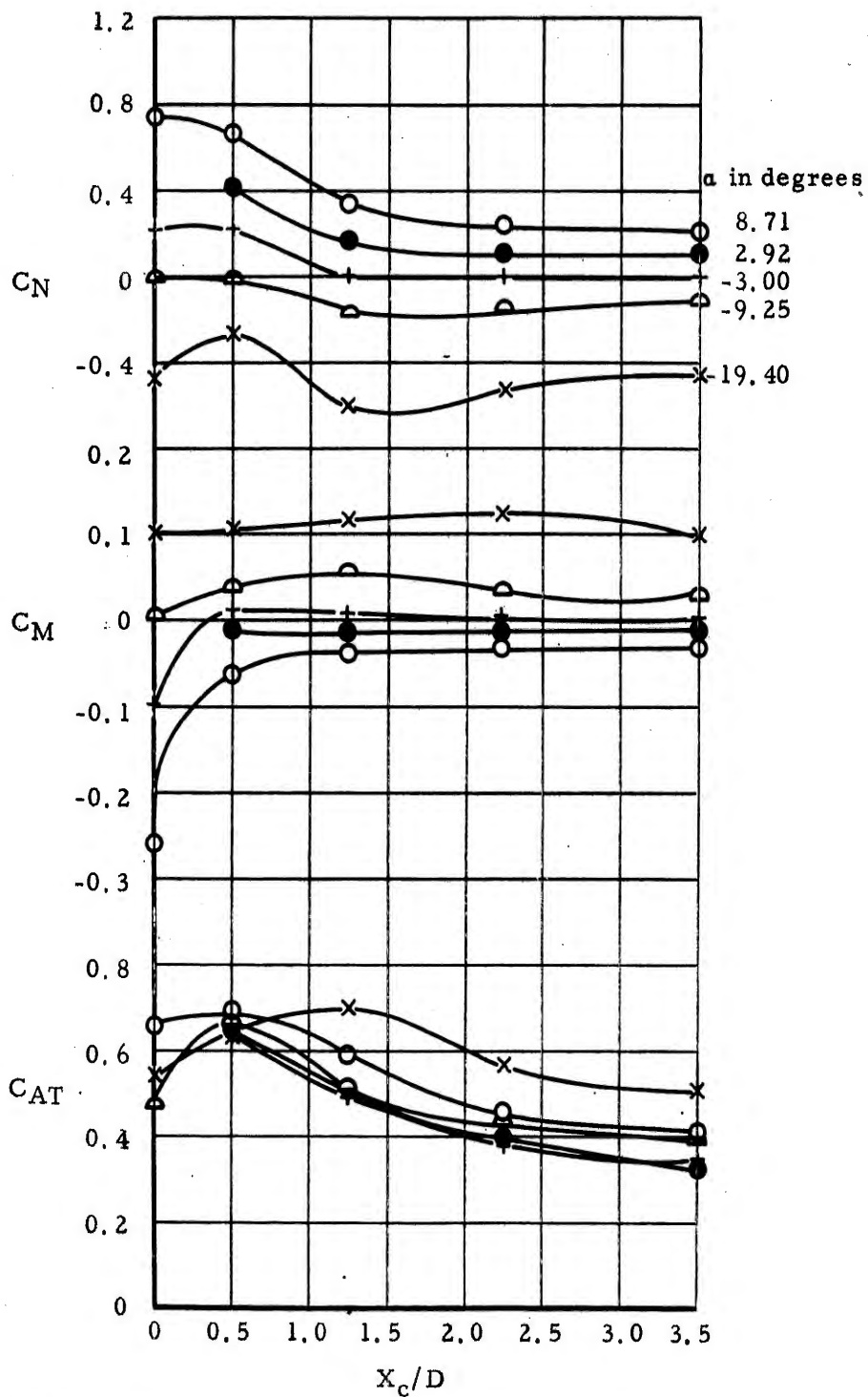


Figure 6d. Close-in Data - Variation of Capsule Characteristics with Axial Excursion in the Carrier Flow Field - Lateral Station $Y_c/D = 1.125$

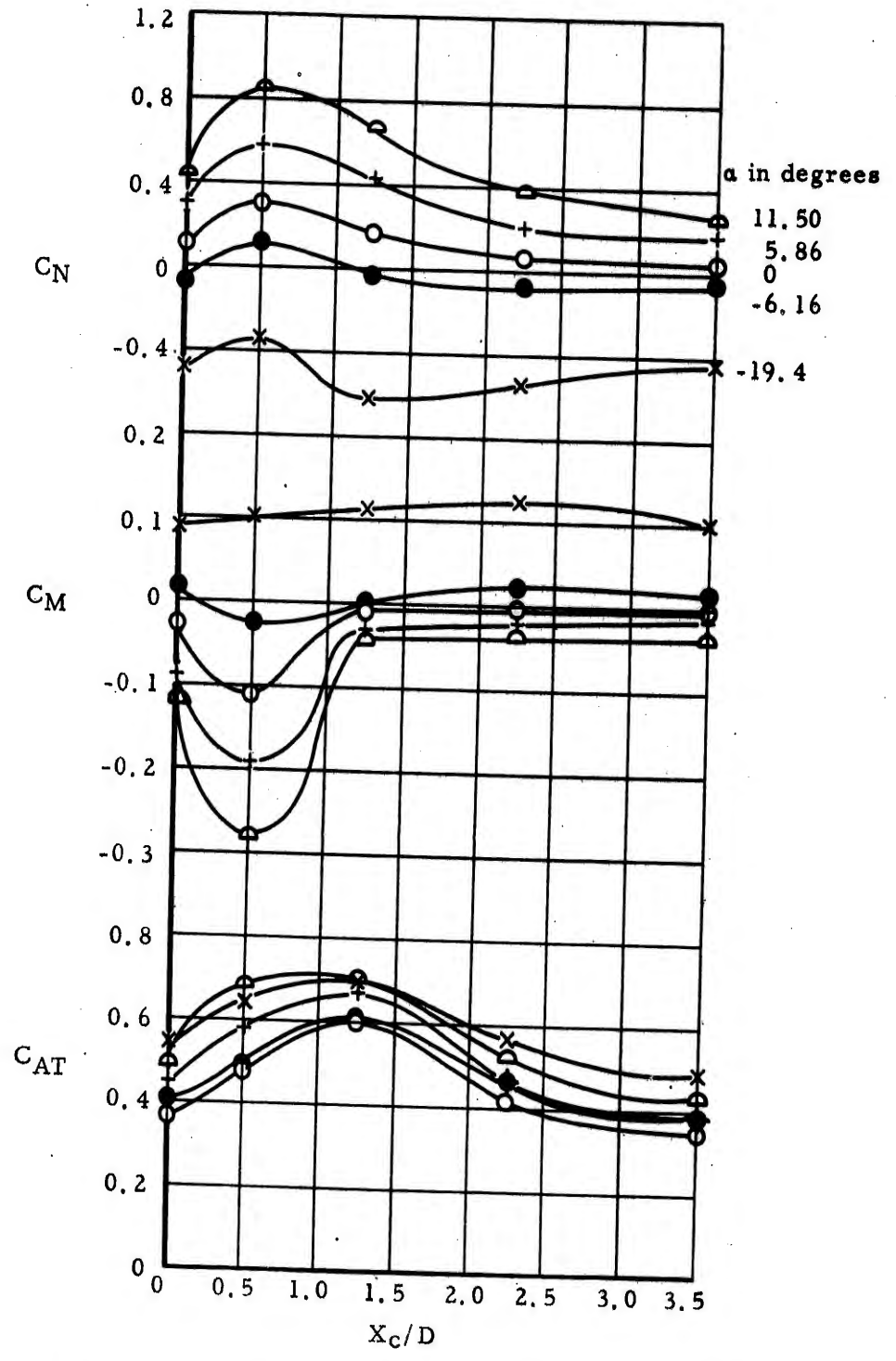


Figure 6e. Close-in Data - Variation of Capsule Characteristics with Axial Excursion in the Carrier Flow Field - Lateral Station $Y_c/D = 1.25$

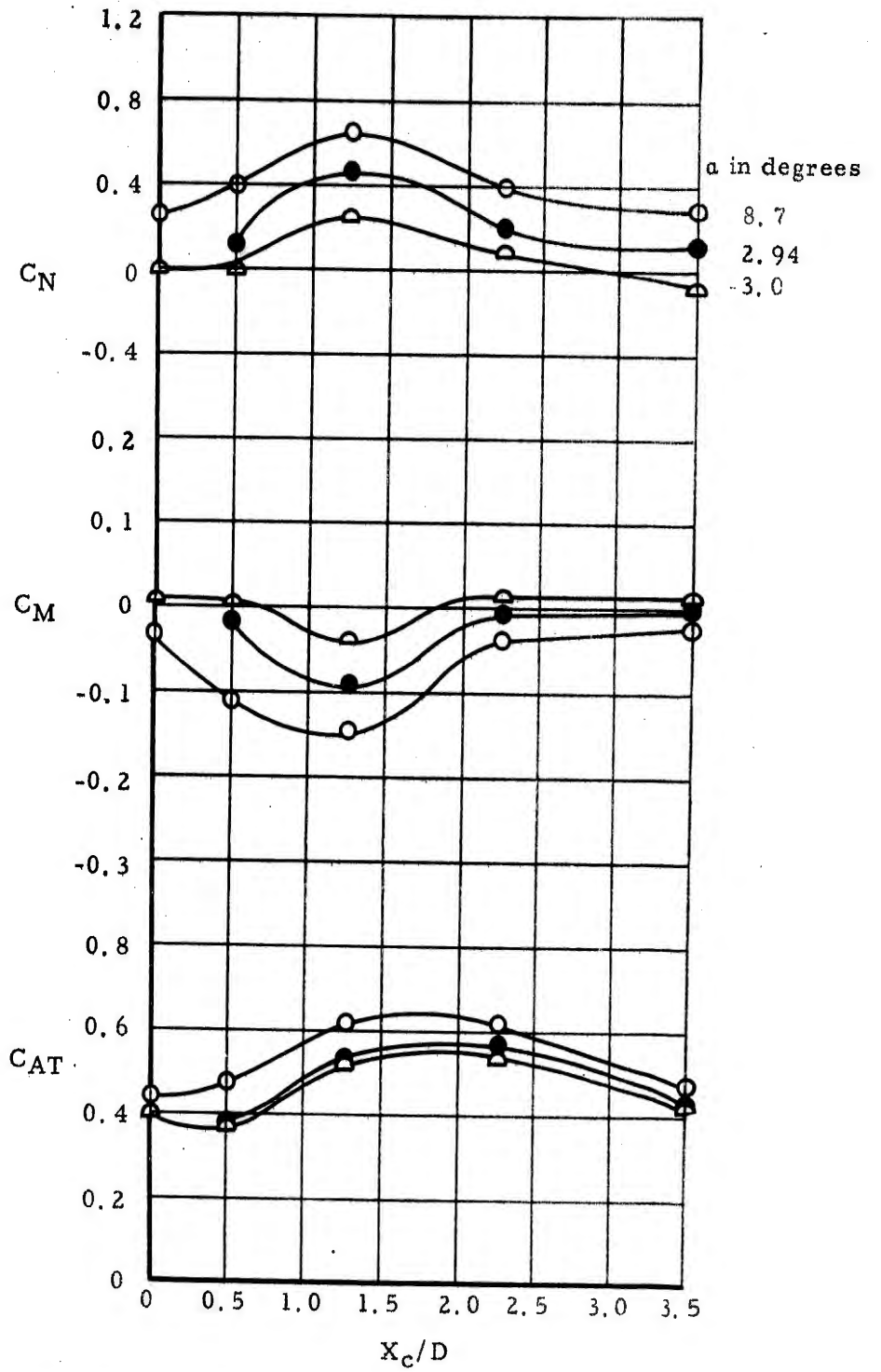


Figure 6f. Close-in Data - Variation of Capsule Characteristics with Axial Excursion in the Carrier Flow Field - Lateral Station $Y_c/D = 1.375$

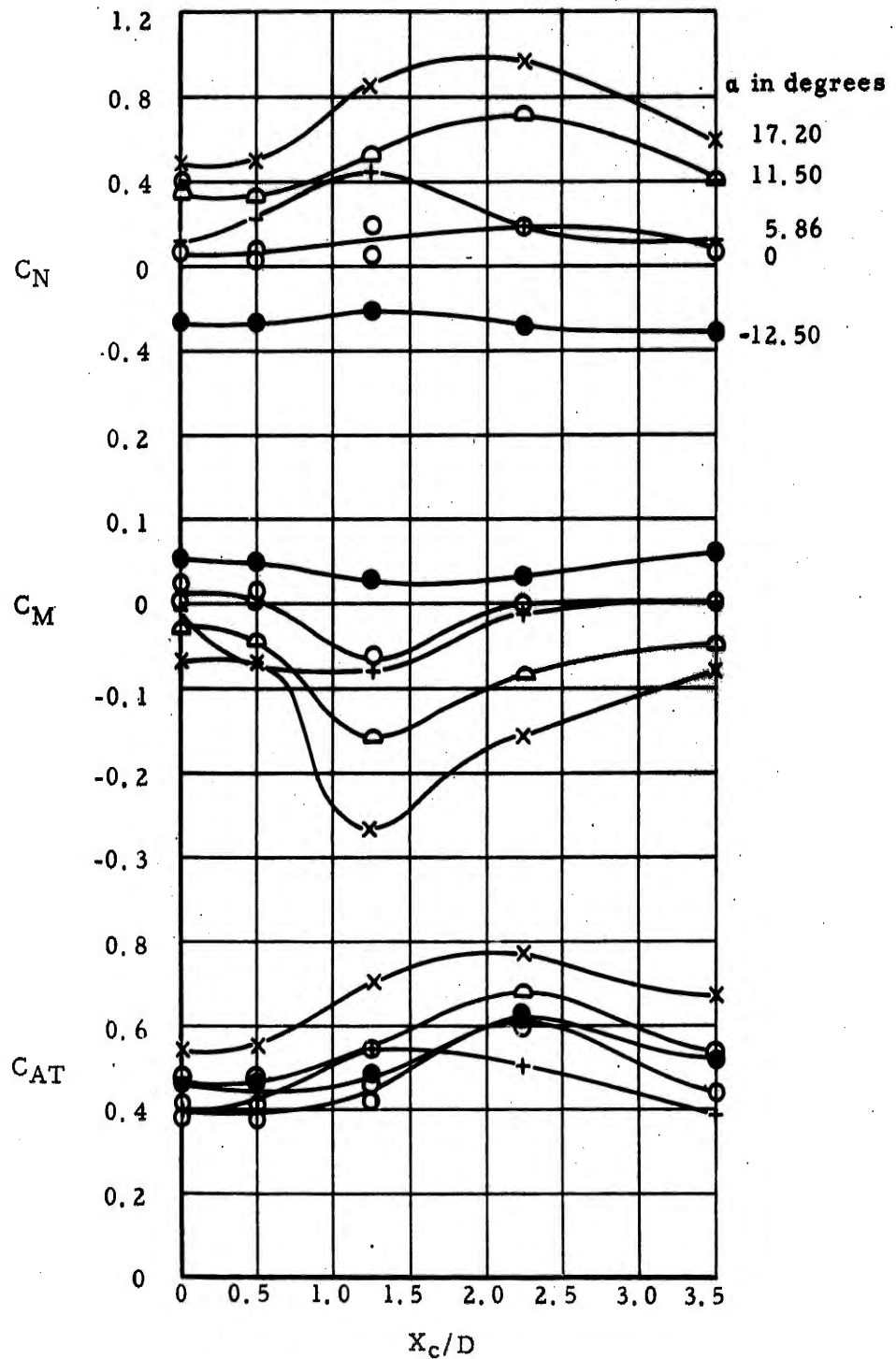


Figure 6g. Close-in Data - Variation of Capsule Characteristics with Axial Excursion in the Carrier Flow Field - Lateral Station $Y_c/D = 1.50$

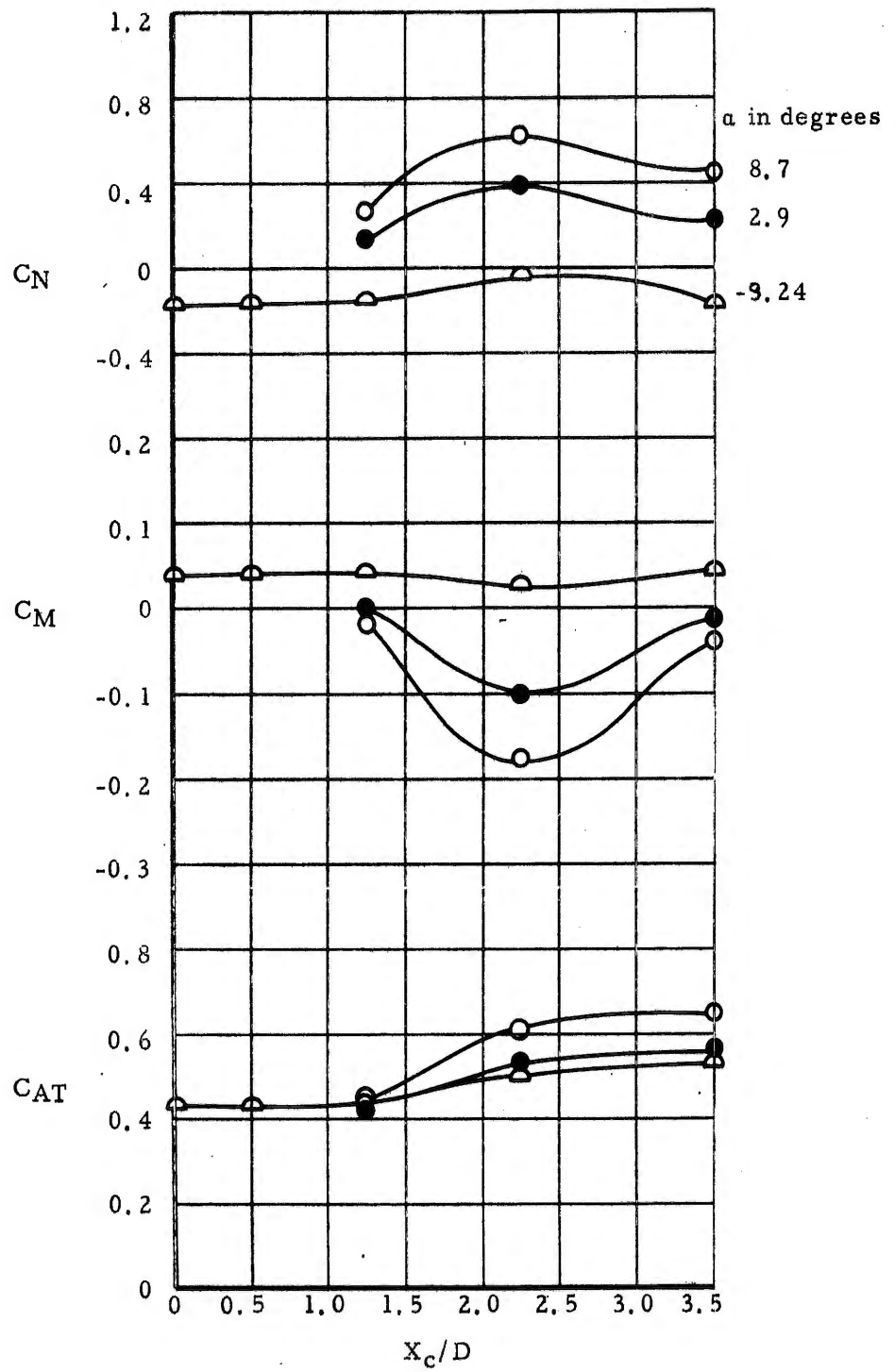


Figure 6h. Close-in Data - Variation of Capsule Characteristics with Axial Excursion in the Carrier Flow Field - Lateral Station $Y_c/D = 1.625$

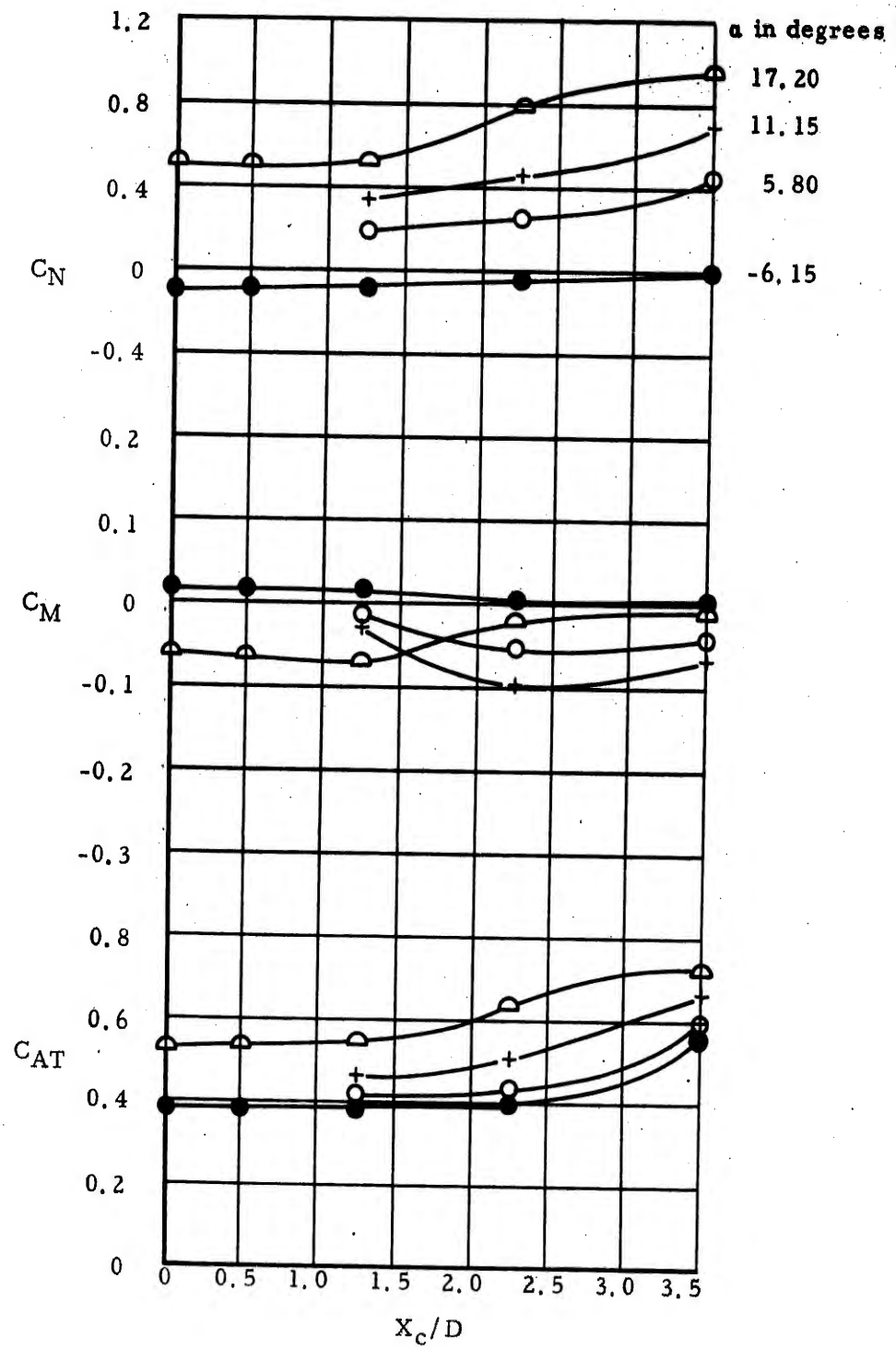


Figure 6i. Close-in Data - Variation of Capsule Characteristics with Axial Excursion in the Carrier Flow Field - Lateral Station $Y_C/D = 1.75$

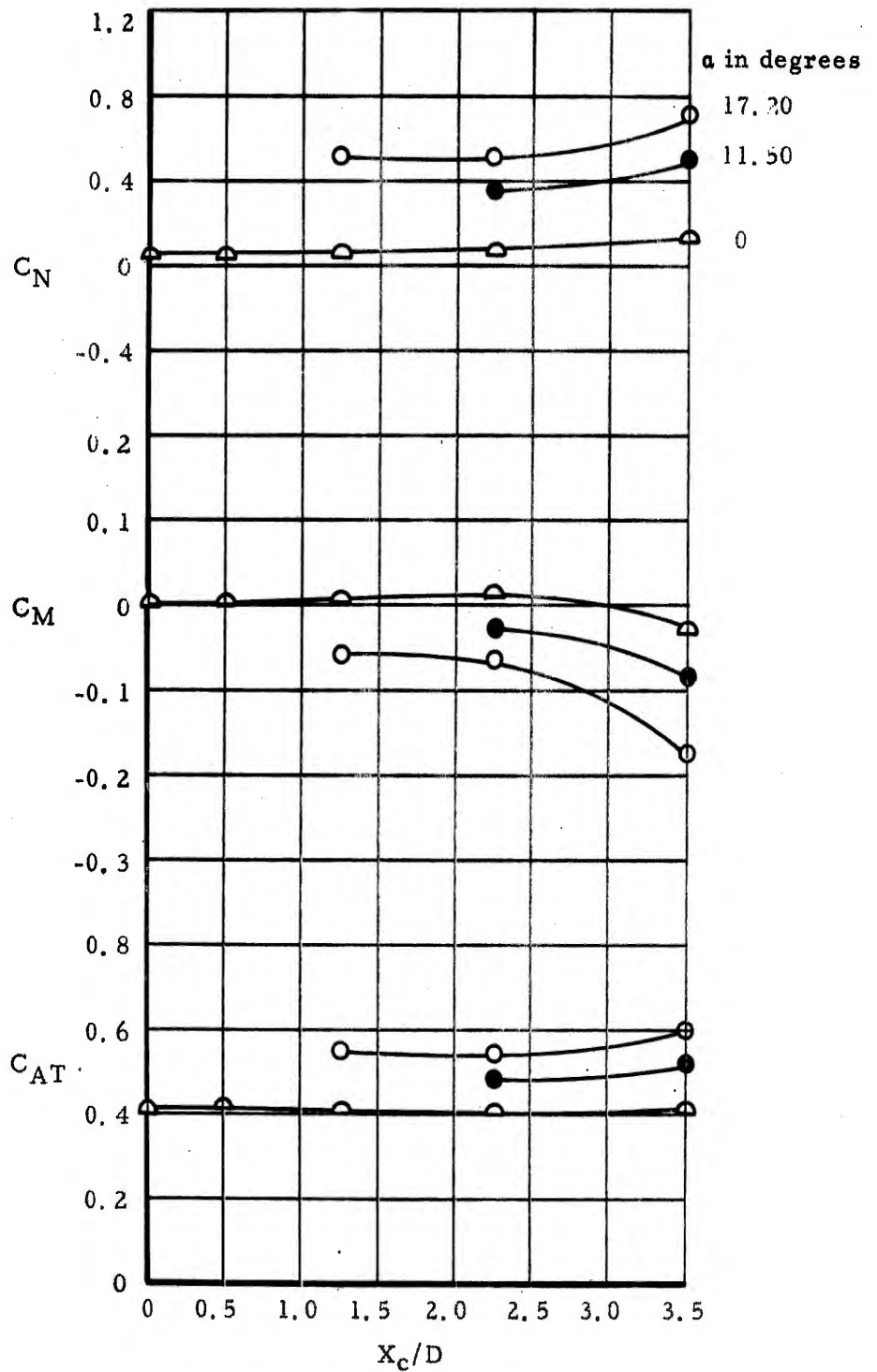


Figure 6j. Close-in Data - Variation of Capsule Characteristics with Axial Excursion in the Carrier Flow Field - Lateral Station $Y_c/D = 2.0$

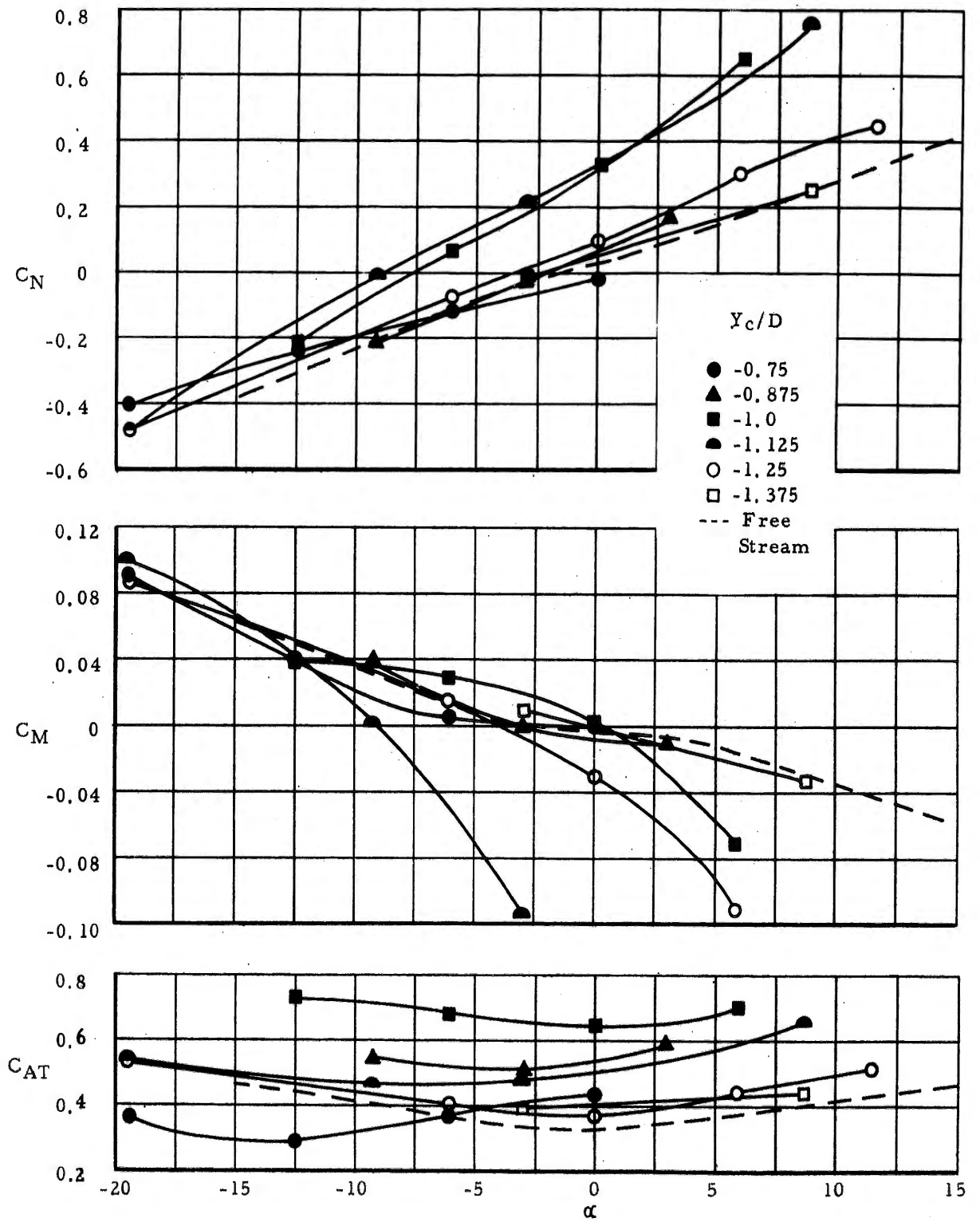


Figure 6k. Close-in Data - Variation of Capsule Characteristics with Angle of Attack at Specified Values of Y_c/D , Axial Station $X_c/D = 0$

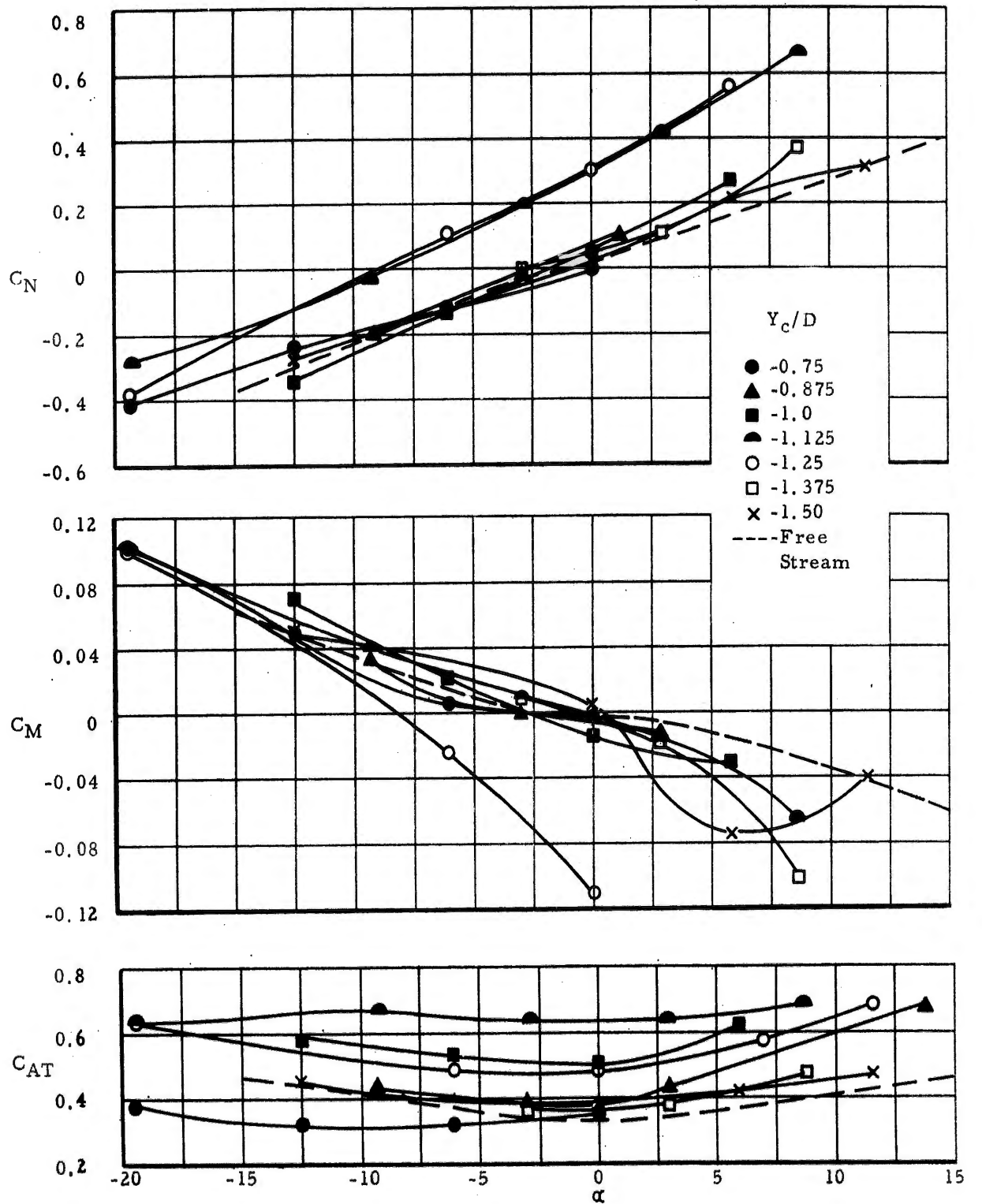


Figure 61. Close-in Data - Variation of Capsule Characteristics with Angle of Attack at Specified Values of Y_C/D , Axial Station $X_C/D = .5$

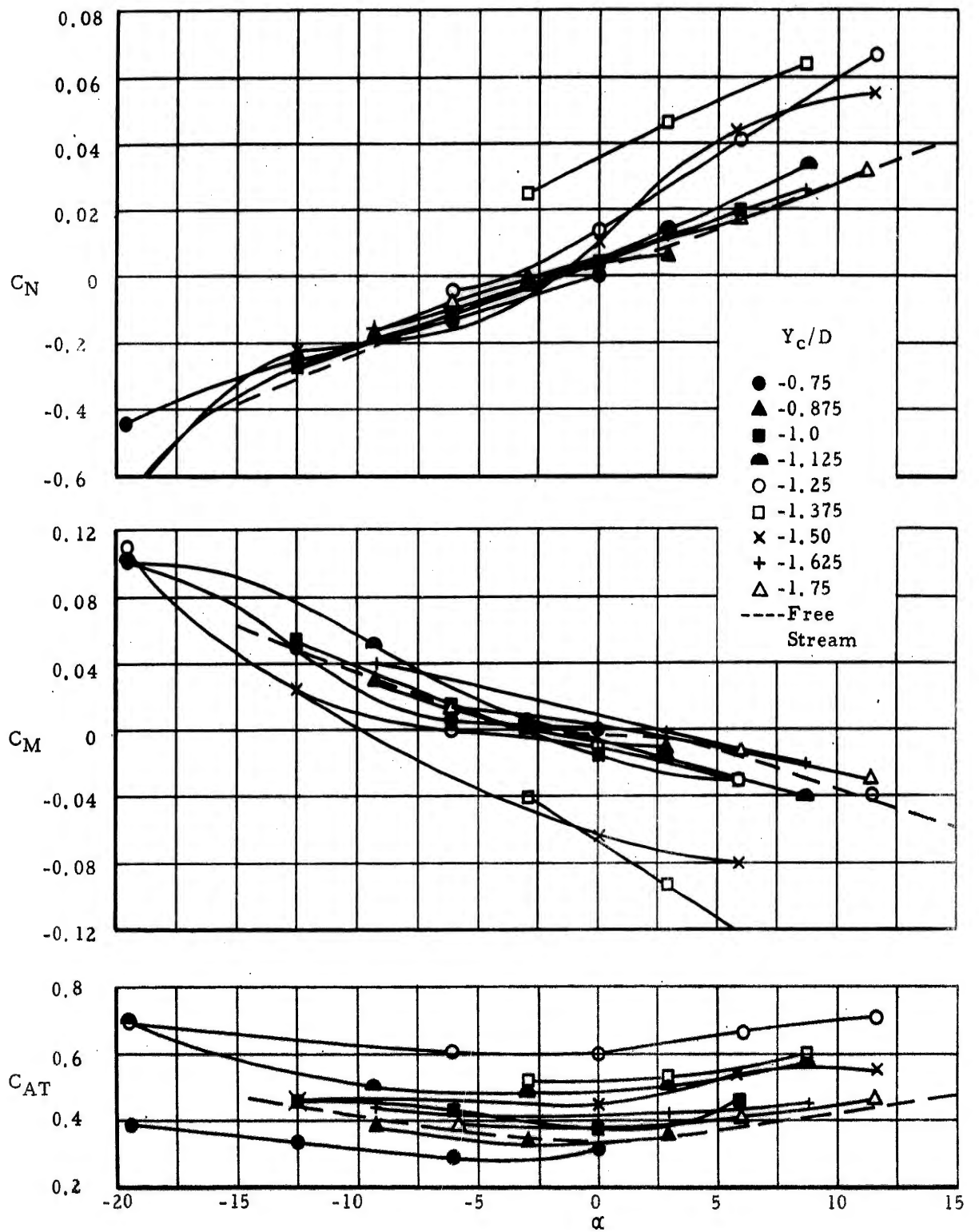


Figure 6m. Close-in Data - Variation of Capsule Characteristics with Angle of Attack at Specified Values of Y_C/D , Axial Station $X_C/D = 0.75$

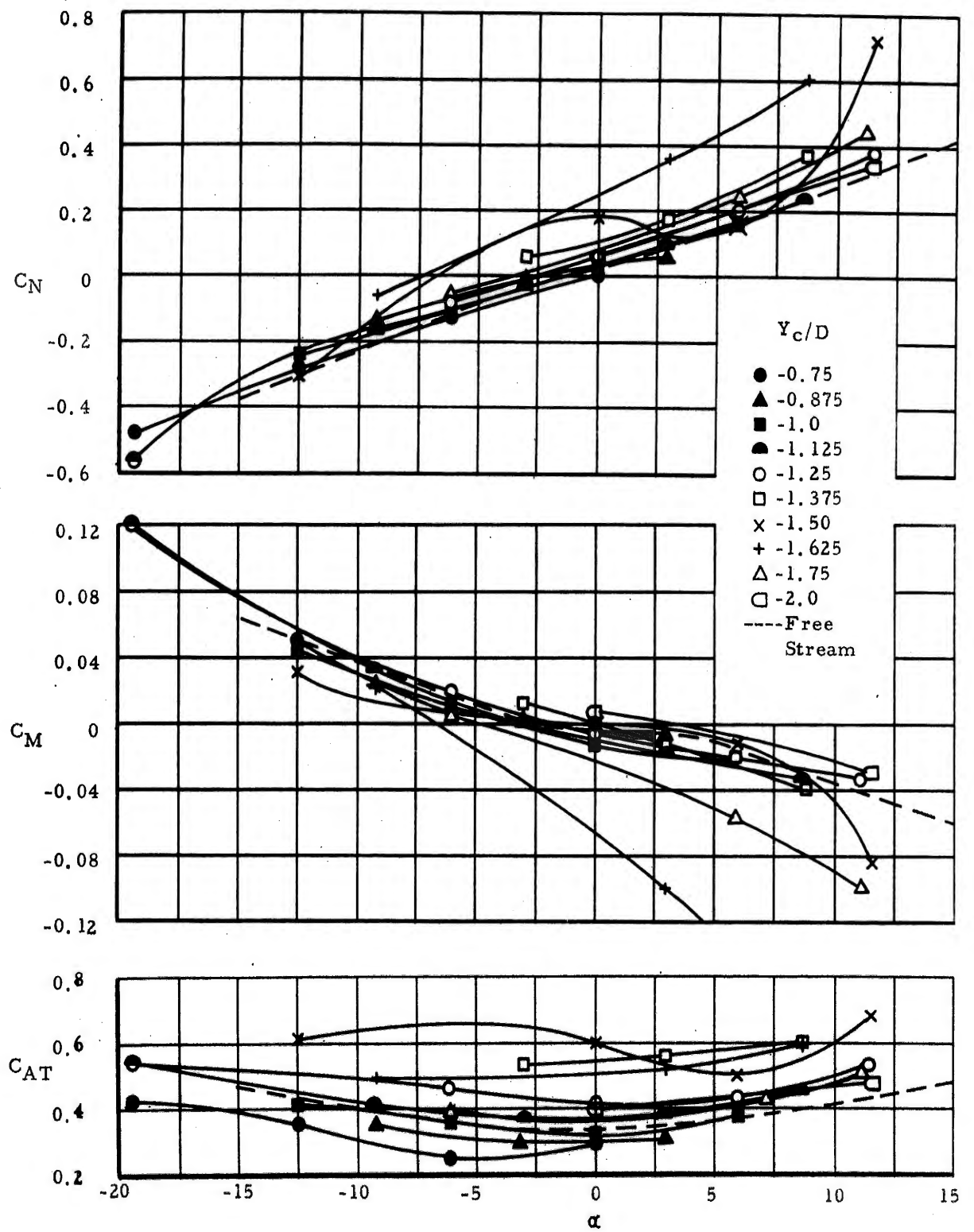


Figure 6n. Close-in Data - Variation of Capsule Characteristics with Angle of Attack at Specified Values of Y_c/D , Axial Station $X_c/D = 2.25$

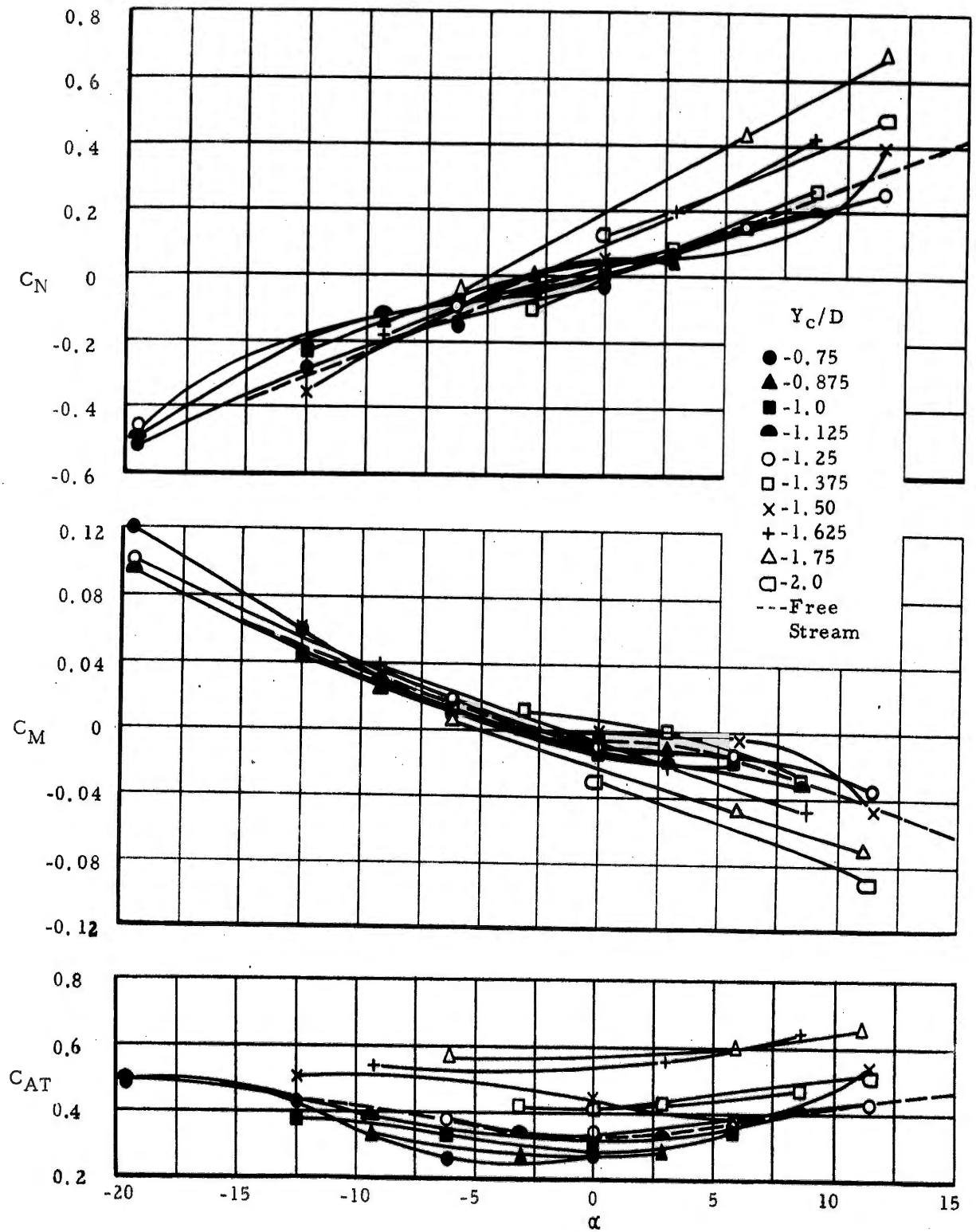
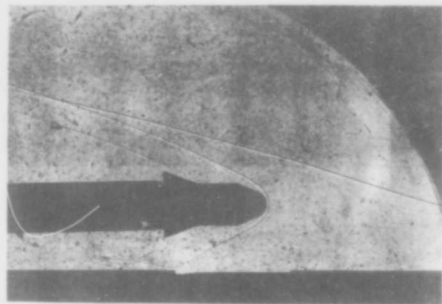
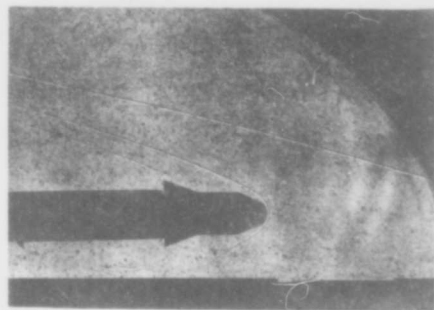


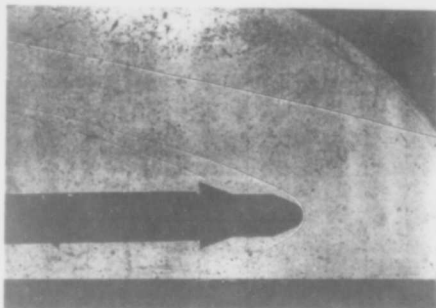
Figure 60. Close-in Data - Variation of Capsule Characteristics with Angle of Attack at Specified Values of Y_c/D , Axial Station $X_c/D = 3.5$



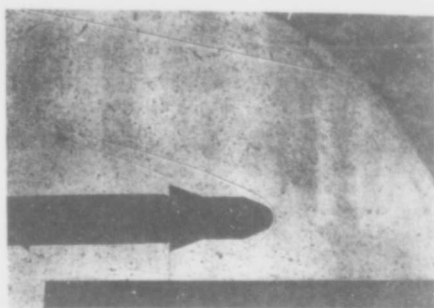
(a) $X_c/D = 0$



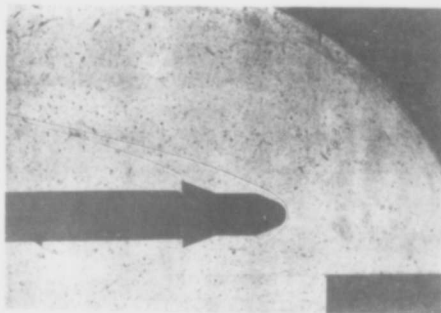
(b) $X_c/D = 0.5$



(c) $X_c/D = 1.25$

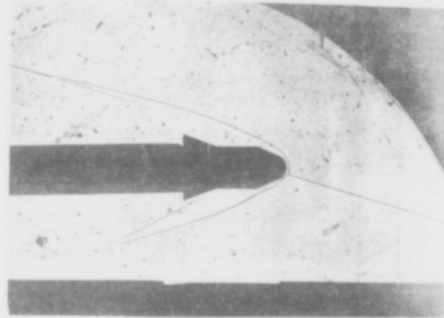


(d) $X_c/D = 2.25$

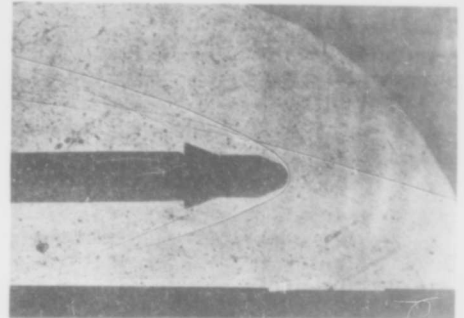


(e) $X_c/D = 3.5$

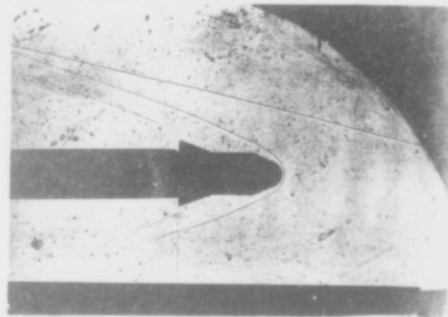
Figure 7a. Close-in Phase - Shadowgraph Sequence Showing Axial Travel of Capsule At Lateral Separation $Y_c/D = 0.75$, $\alpha = 0$



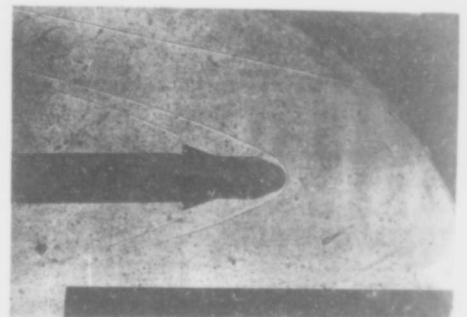
(a) $X_c/D = 0$



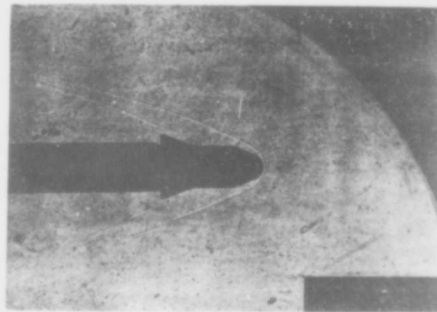
(b) $X_c/D = 0.5$



(c) $X_c/D = 1.25$



(d) $X_c/D = 2.25$



(e) $X_c/D = 3.5$

Figure 7b. Close-in Phase - Shadowgraph Sequence Showing Axial Travel of Capsule At Lateral Separation $Y_c/D = 1.00$, $\alpha = 0$

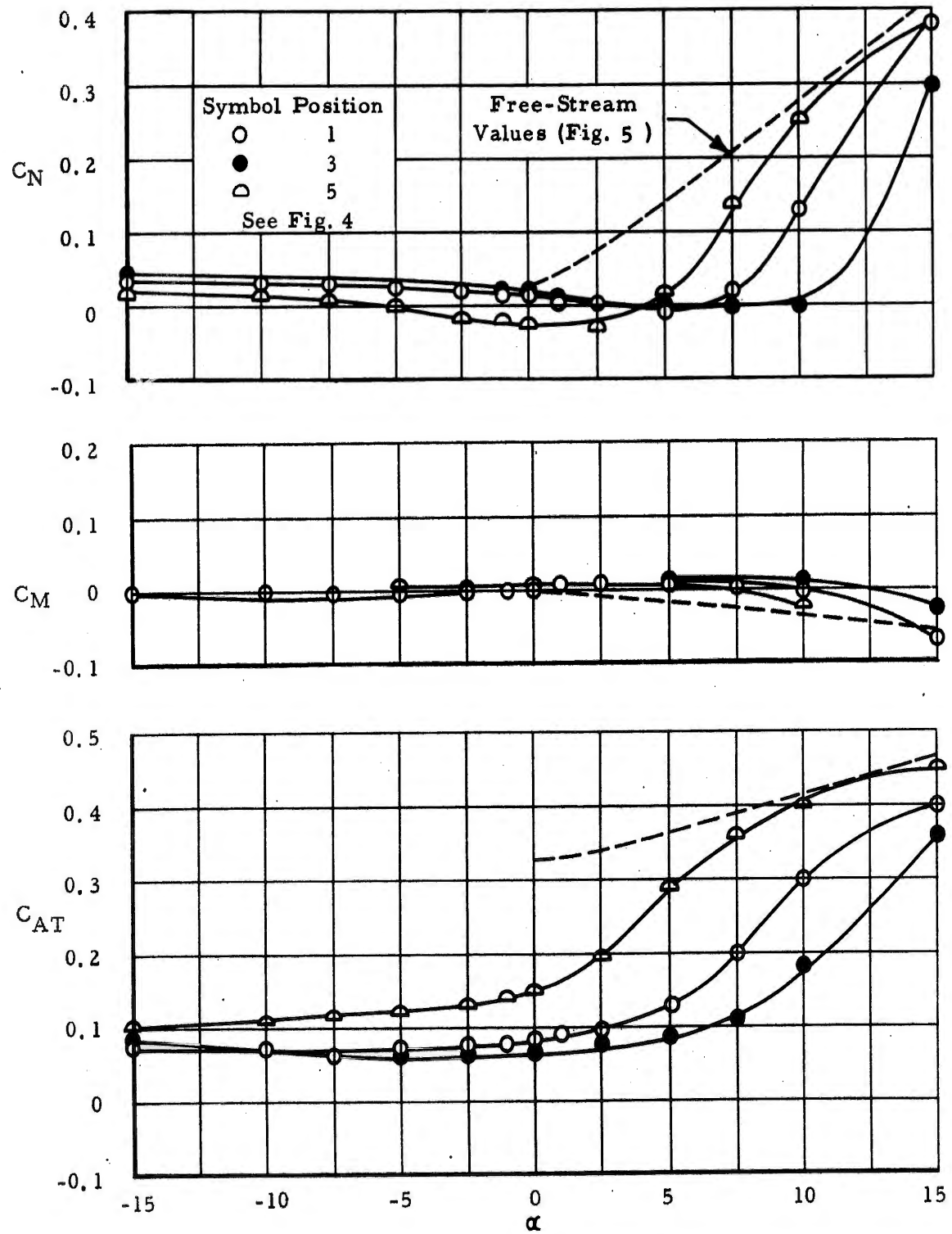


Figure 8a. Capsule Penetration of the Wake Boundary

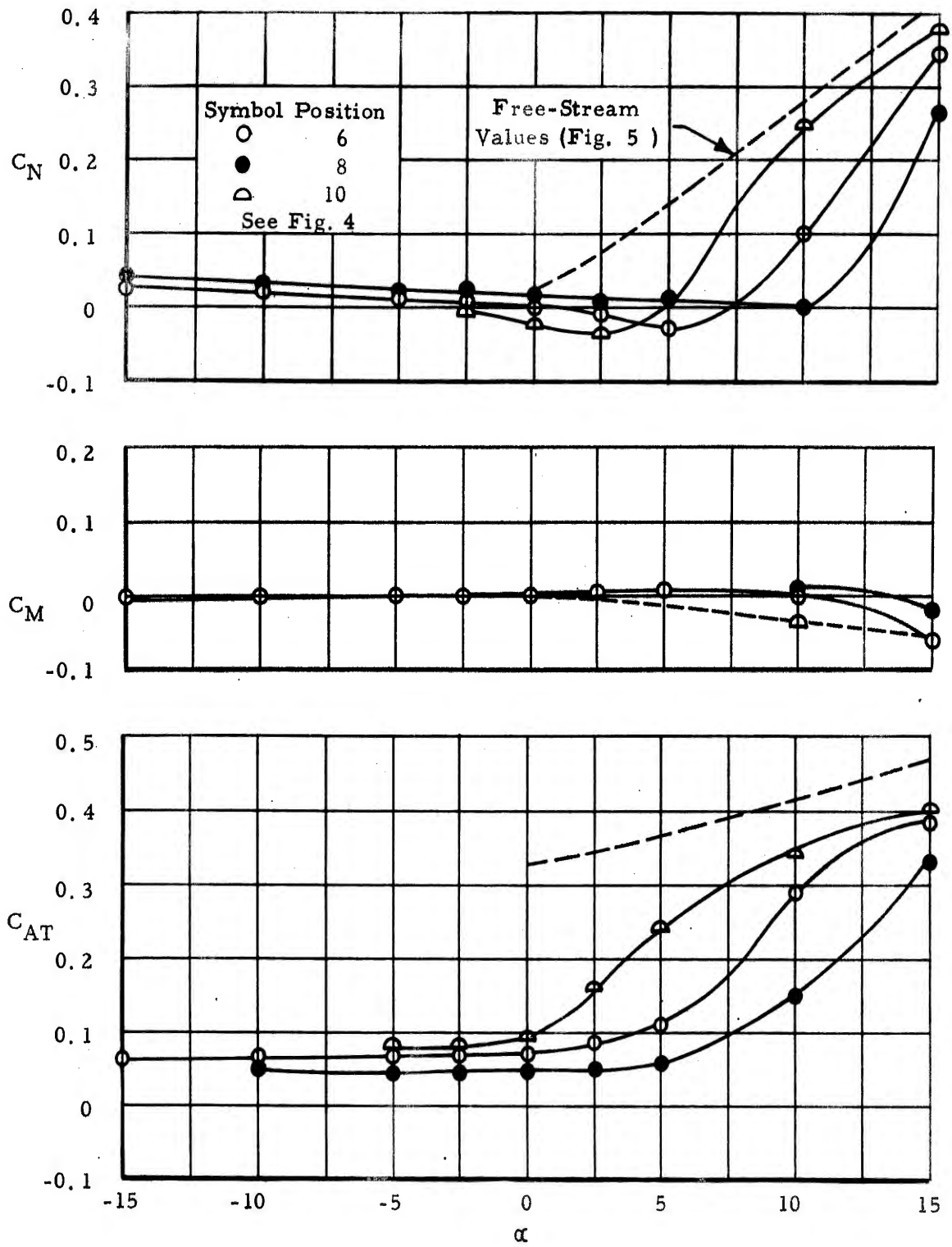


Figure 8b. Capsule Penetration of the Wake Boundary

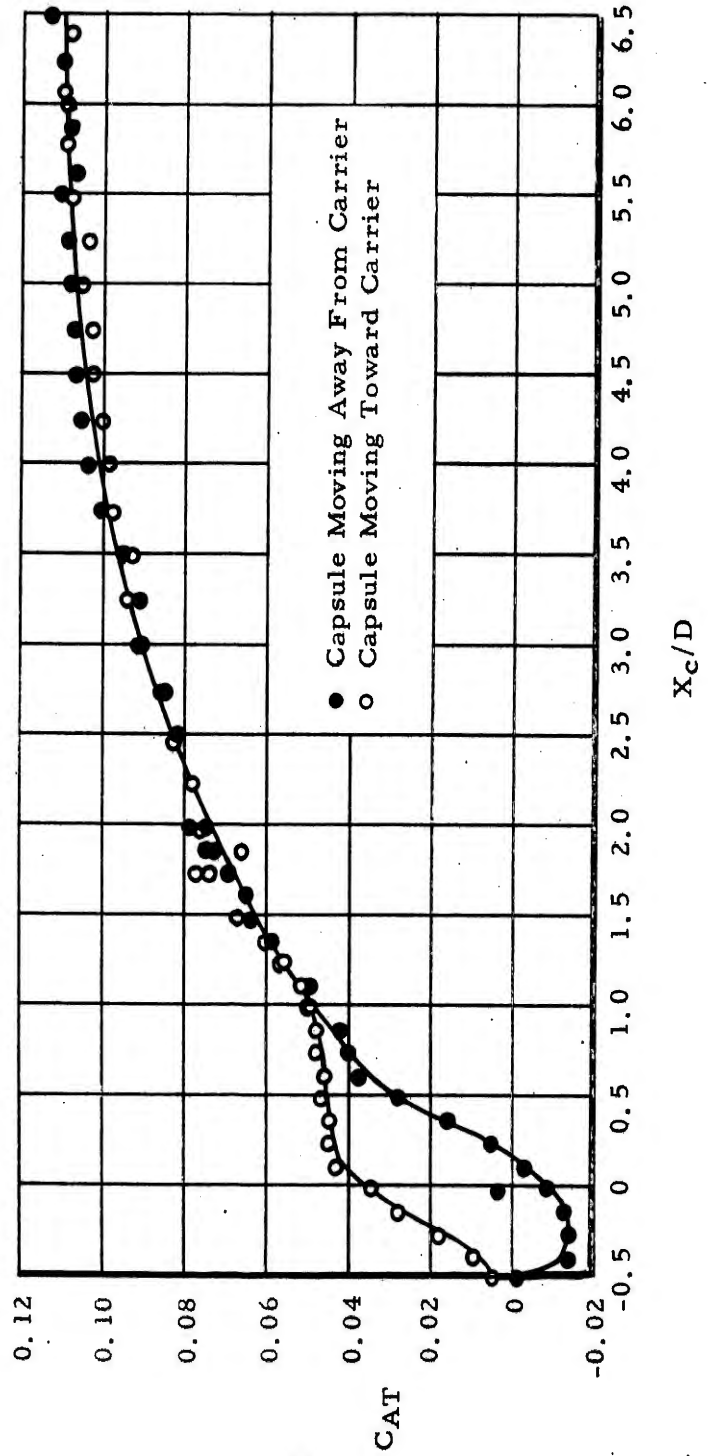


Figure 9a. Variation of Axial Force Coefficient Along the Carrier Wake Axis for a Free Stream $Re = 3.36 \times 10^6$ /Ft.

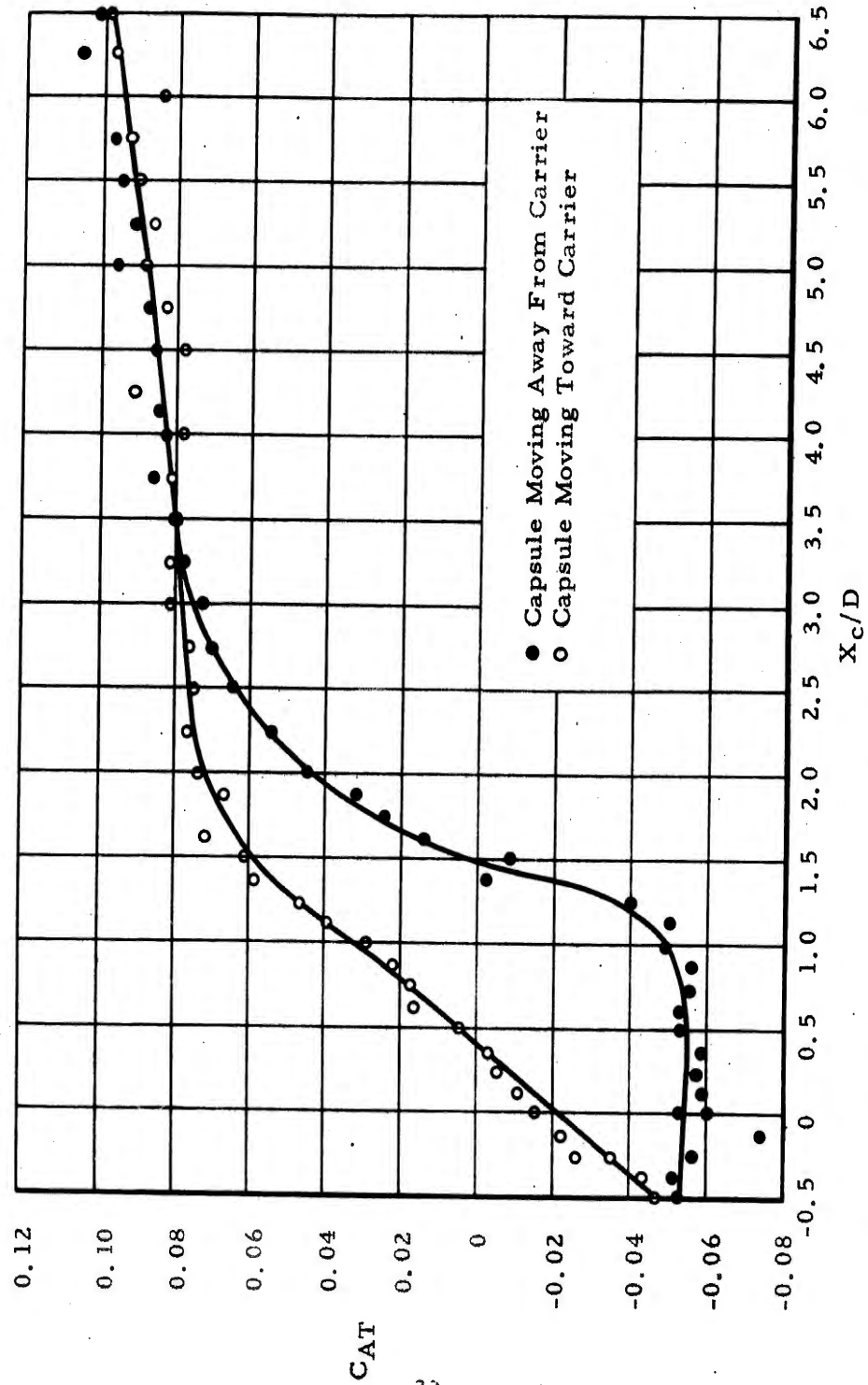


Figure 9b. Variation of Axial Force Coefficient Along the Carrier Wake Axis for a Free Stream $Re = 1.69 \times 10^6$ /Ft.

SECTION IV

DATA ANALYSIS

The test data obtained have been studied to determine the trends of variations and the local flow conditions that would be necessary to produce these trends. The data are considered in three main categories; Close-in Effects, Wake Penetration and Wake-Capsule Interaction.

A. Close-In Effects

A study of the close-in data shown in Figures 6a through 6o reveals that when the capsule approaches closely or intersects the carrier bow wave, very pronounced changes occur. This is a critical region for consideration. It will be shown that these changes immediately behind the bow wave are as a result of the local dynamic pressure increase and the local flow inclination away from the carrier axis. Lateral excursions aft of this critical region (fixed Y_c/D location) indicate that the force and moment coefficients tend to approach that of free stream, if not in absolute magnitude at least in flow inclination ($\alpha = 0$).

To evaluate and compare a theoretical procedure to predict these coefficients, a characteristic flow field was generated for a 15° half-angle cone cylinder body combination. It should be noted that in these calculations, the body assumed was a pointed cone as opposed to the blunted cone actually used in the wind tunnel tests (Figure 1). It would be expected that as a result of this configuration difference, the capsule characteristics close in to the carrier vehicle, that is Y_c/D equal 0.75 may well differ from those obtained in wind tunnel tests. Figure 10 shows a comparison of the predicted shock wave location versus X/D as obtained from the characteristic program and that obtained from the measurements of shadowgraph photographs obtained from the tests. It is seen that very good agreement is obtained between the predicted and recorded shock wave locations. This agreement excluding the effects of vorticity induced by the flow field near the body, would indicate that for the larger Y/D locations the flow field obtained in the wind tunnel tests should agree with those obtained from the generated flow field.

Using the results of the characteristics generated flow field, capsule coefficients were estimated for some of the same Y_c/D , X_c/D , and angles that were obtained in the wind tunnel program. Figures 11a through 11d show the results obtained. In computing these coefficients, the effect of dynamic pressure ratio, local Mach number, and flow inclination at the mid-point of the capsule were used. No attempt was made to account for the gradients in the above parameters that certainly do exist near the shock wave.

In the computations of the capsule coefficients, use of the previously reported free stream data for normal force and moment coefficient at Mach numbers of 2, 3, 4, and 5 were used to evaluate the local Mach number coefficients. For the axial force coefficients, it was found that for the Mach 8 tests the axial force coefficient is approximately 13 percent higher than the value reported in Volume II at a Mach number of 5 for the small capsule. This rise in axial force coefficient with increasing Mach number is contrary to the trend of published data for cone-cylinder-flared bodies (Ref. 3) excluding the effects of Reynolds number. As a result of the deviation from established trends for this type of shape, the following approximations have been used in an attempt to correct for what is apparently a low Reynolds number effect. Figure 12 shows the curve of axial force coefficient versus Mach number for zero angle of attack and the data points obtained from tests using the 0.8 inch cylindrical diameter model used in this program, and a model whose cylindrical section was 6 inches in diameter (Volume II, Ref. 1). For angles of attack greater than zero, values were interpolated between the approximate curves shown for $\alpha = 5, 10$ and 15 degrees.

In Figures 11a and 6a, which show the predicted coefficient and data for Y_c/D equal to 0.75, it is seen that the predicted values of C_N and C_M for the low angles agree extremely well with the data. For the -19.4° angle of attack, both C_N and C_M deviate appreciably at the most aft X/D location. This trend is probably in part due to the flare portion of the capsule extending into a higher energy air flow (away from the body) and hence, being subject to larger forces than that which would be associated at $Y_c/D = 0.75$.

The predicted axial force coefficient variation at this Y/D location is significantly different from the data for the low angles of attack at the forward X_c/D locations and completely different in trend at the high angles. The trend exhibited by the data for low angles is the same as that predicted; however, the magnitude with decreasing X_c/D is not adequately predicted. This deviation, as was stated earlier, may well be due to the difference in geometry of the characteristic flow field carrier from that of the wind tunnel model since the axial force coefficient magnitude is highly dependent on Mach number. The reversal in axial force trend of the high angle data is again consistent with the effect described above for the normal force and moment coefficient. In general for capsules at low angles, the predicted results are in good agreement for this Y_c/D location.

Figures 11b and 6c show the predicted coefficients and test data for a Y_c/D of 1.00. It is noted that for this Y_c/D location, the nose of the capsule is in the carrier vehicle shock wave at X_c/D equal to 0 (Figure 7b).

For this Y_C/D location, the predicted values of C_N and C_M are in reasonable agreement for all angles except +5.86 degrees which differs slightly at large X_C/D locations for C_N and is significantly different in C_M at 0 and 0.5 X_C/D . The deviation in the values of C_M can most likely be attributed to gradient effects due to the shock wave curvature and the flare of the capsule being further away from the large flow inclination angles that are predicted by using the middle of the capsule for local flare properties.

The axial force coefficient trend with X_C/D is fairly well predicted; however, in all traverse locations except 0 (nose of the capsule immersed in the shock wave) the axial force coefficient is considerably lower than recorded in the data. This deviation in axial force coefficient on the average is approximately 0.05.

Figures 11c and 6e show the predicted coefficients and test data for a Y_C/D of 1.25 and various X_C/D 's. Comparison of these two figures shows that extremely good agreement on the whole is obtained for all angles for C_N . The values of C_A differ in absolute magnitude at various X_C/D locations which in part could be associated with the assumed axial force coefficient variation with Mach number (Fig. 12); however, the trends for the various angles are quite closely predicted.

The values of C_M are predicted reasonably well at X_C/D of 3.5. However, as the capsule is moved forward in the interference flow field, specifically for large positive angles, the values of C_M predicted overestimate the restoring moment of the capsule. This effect is again probably attributable to the fact that the gradient in flow field angles is most pronounced near the shock wave and the flared portion of the capsule would be farther away from the shock wave for high positive angles.

The predicted and test data for a Y_C/D of 1.5 and X_C/D 's of 2.25 and 3.5 are shown in Figures 11d and 6g. Comparison of the test data and predicted values of C_N for the five angles shown indicates very good agreement except for an angle of +5.86 degrees. The coefficients obtained for this angle at all X_C/D locations show erratic tendencies and the coefficients do not conform to any of the trends for capsule angles above and below this value. Due to this strange behavior of the coefficients for this angle these data have not been weighed heavily in comparing the predicted and read values for C_N , C_M and C_A .

The measured and predicted values of C_M are in far better agreement at X_C/D equal to 3.5 than at 2.25. For the forward region the nose of the capsule is in the shock wave and hence the deviation of the predicted and

measured values would be expected by ignoring the flow field gradients. It is noteworthy, however, that the effect of the shock wave impinging on the nose of the capsule does not alter the trends obtained by the prediction technique.

The predicted values of C_A compare with the test data in the same manner as do the values of C_M discussed above. It is expected that better agreement with the data could be obtained in these areas if the strip theory or the procedure outlined by Moskowitz (Ref. 4) as discussed in Volume II were used.

B. Wake Penetration

The wake penetration data obtained at a Mach number of 8.09 are shown in Figures 8a and 8b. It is seen in both figures that the change in coefficients with angle (which corresponds to a change in X_c/D and Y_c/D as shown in Figure 4) is quite uniform and no large discontinuities are experienced as the capsule is translated through the wake boundary. In all cases, the trends exhibited by the data are consistent with a qualitative description of the wake geometry given in Volume I (Ref. 5). Examples of this type of agreement are the increased magnitudes of the force coefficients at zero angle at the outer position points (5 and 10) compared to the corresponding lower position points. It is further seen that at the outer data positions at zero angle, the flow has expanded around the base of the vehicle since negative normal force coefficients are obtained.

An attempt has been made to correlate the results of these data with the wake convergence angle given by Love in Ref. 6. The procedure used in Volume II, Ref. 1 to compare the results with the Love prediction was to determine the angle where the capsule normal force coefficient was zero when the capsule was on the edge of the wake boundary. This procedure is not applicable for these data since the capsule's angle relative to the carrier vehicle's longitudinal axis was small ($\pm 5^\circ$) when the capsule was positioned on or near the edge of the wake boundary. When the capsule is rotated to the range where reasonable agreement with the predicted value (13.5°) could be obtained the capsule center of gravity was approximately 1 caliber off the carrier's longitudinal axis. At this point, the capsule will be in the middle or completely out of the expansion fan and hence, the local flow deflection it is subjected to is not that at the wake boundary. In light of the above discussion, the axial force coefficient was considered for detecting the wake boundary. The assumption used for this technique is based upon the criterion that a significant rise in axial force should accompany the capsule's penetration of the wake boundary. Based on this assumption, the following capsule c. g. coordinates associated with capsule angles were used in obtaining a predicted wake boundary.

<u>Capsule Position at Zero Angle (Point No.)</u>	<u>Capsule Angle (Degrees)</u>
1	0
3	+ 2.5
5	- 2.5
6	0
8	+ 2.5
10	-2.5

The results of the above procedure rendered an expansion angle of 11.5 degrees as compared to a predicted value of 13.5 by Love. This discrepancy could be accounted for by the fact that the capsule would be at an angle relative to the flow of at least 9 degrees if 11.5 degrees is assumed, and possibly 16 degrees if the predicted value of 13.5 degrees is correct. This inclination of the flow field relative to the capsule could possibly alter the shape of the wake as discussed in Volume II and hence, account for the variation in the wake expansion angles discussed above.

Since the side flow field data discussed previously (in A, Close-in Effects) are in reasonable agreement with predictions, it is expected that reasonable predictions of the capsule coefficients could be made for the capsule outside the wake boundary using an expansion angle given by Love and empirically fitting the values at the wake boundary and those on the wake core for the Reynolds number conditions which are appropriate with the data.

C. Wake-Capsule Interaction

Figures 9a and 9b show the capsule axial force coefficient variation based on free stream dynamic pressure and flare base area for various capsule locations in the carrier vehicle wake at two tunnel Reynolds numbers. It is noted that for these data the origin of the axis is the base of the carrier vehicle and all measurements are referenced to the nose of the capsule. All the force measurements made were with the capsule's axis aligned with the carrier vehicle's longitudinal axis.

The wind tunnel conditions for which these data were obtained were 8.09 Mach number and total pressures of 800 and 400 pounds per square inch. The free stream Reynolds numbers for the two total pressures are 3.36×10^6 and 1.69×10^6 per foot, or referenced to the cylindrical section of the capsule, 2.24×10^5 and 1.13×10^5 , respectively.

The variation of the axial force coefficients with axial distance behind the carrier is due primarily to the variation of effective wake Mach number, dynamic pressure, and for the close-in region, a static pressure variation. Comparison of the two Figures, 9a and 9b, indicates that aft of approximately 3.0 calibers the two curves are similar and deviate from each other by approximately 0.015. Forward of this axial location however, the two curves deviate from each other significantly for the data points where the capsule is moving aft in the wake (away from the carrier vehicle). It is noted that the curve shown through the data points given by circles or capsule moving toward the vehicle, are consistent with trends exhibited by data in Ref. 7 where a rigid cone was traversed through the wake of a carrier vehicle. In all the above-mentioned data, this hysteresis effect is quite pronounced. It is doubtful as to whether any important significance can be given the more favorable axial force curve given by the capsule moving toward the vehicle until the capsule has passed the region where the two curves are common. This portion of the curve has not been considered for any empirical representation for ejection velocity requirements in this report and is considered of only academic interest for wake core deployments until knowledge of the underlying principles of the hysteresis effect are more firmly known, can be predicted analytically or shown to be applicable when the dynamic behavior of the capsule is considered.

Figure 13a shows the comparison of the high Reynolds number data with a prediction technique described in Volume II, Ref. 1. This technique employs an empirical fit to subsonic turbulent analysis for basic functional variations in wake properties with longitudinal and transverse distances aft of the close-in portion of the wake. In the prediction technique, the average dynamic pressure and average Mach number across the positions of the wake occupied were computed ignoring possible capsule-wake interaction and longitudinal gradients. In all cases, the midpoint of the capsule was used in determining the local effective Mach number and dynamic pressure. The values of $C_{Aa} = 0$ used for the capsule at the various local Mach numbers, are shown in Figure 12.

It is seen in Figure 13a that for the aft portion of the wake (X_c/D greater than 1.2 calibers) the predicted curve deviates from the data by less than 0.06 in drag ratio. This discrepancy occurs at the minimum wake thickness and could logically be explained by the fact that the prediction technique does not account for the gradients in Mach number, dynamic pressure, as well as static pressure which do exist. It is of interest, however, that the technique used correctly predicted the Mach 4 data in Volume II to have a wake to free stream drag ratio of 0.66 at 6 calibers and 0.35 at Mach 8.

In the close-in position, Figure 9a, negative axial forces are indicated by the data. The predicted curve in this region uses (1) the above-mentioned procedure for the region where the effect produces a positive axial force, and (2) an extrapolation of data presented in References 6 and 8 which show the existence of an increasing static pressure with distance behind an axially symmetric body. It is seen that the technique deviates from the data by a significant amount at 0.5 calibers; however, the deviation is in a direction as to produce conservative estimates of the required ejection velocity to effect separation of a capsule.

Figure 9b shows the comparison of a predicted curve with the test data for a Reynolds number of 1.69×10^6 per foot. For these data, it appears that a significant shift in the minimum wake thickness location has occurred as compared to the test data described above. To obtain the predicted curve shown, it was necessary to make the premise that for this Mach number-Reynolds number combination, a rearward movement of the wake minimum thickness location is feasible. This premise is, to some extent, justified if it is assumed that the carrier vehicle boundary layer is laminar or in transition (i. e., boundary layers unable to sustain a large adverse pressure gradient) at the vehicle base since the argument advanced by Love (Ref. 6) for turbulent boundary layers indicates that the expansion angle at the base of a vehicle is governed by the pressure gradient, the flow can negotiate when compressed by the trailing shock.

Based on this assumption and the agreement of the prediction technique for the 3.26×10^6 Reynolds number data, various minimum wake thickness locations were assumed to determine where the best agreement between data and prediction could be obtained. The result of this trial and error solution resulted in a minimum wake thickness location of 2.0 calibers. For close-in region, the same procedure was used as that given for the high Reynolds number data. It is seen that a large disagreement between this procedure and test data occur for X/D locations between 0 and 1.5 calibers. This deviation cannot reasonably be accounted for by a simple horizontal pressure gradient between the base of the capsule and the nose of the capsule since base pressure measurements recorded indicate the capsule base pressure coefficient is negative and a vacuum at the front of the capsule would produce a maximum negative absolute coefficient of less than 0.023. Based on these results, it would be expected that due to a horizontal pressure gradient, the maximum negative axial force coefficient would have to be less than -0.023 as compared to the value of -0.055 recorded in the data. This problem is further aggravated by the fact that if reverse flow is considered as a possible explanation for this deviation, it appears that reverse flow velocities of significantly larger than Mach 1 would be required to account for this deviation. Since this magnitude of reverse flow appears impracticable, a reasonable explanation for these data is not readily available in light of the repeatability of the fore and aft measurement agreement at -0.5 calibers and the agreement of the low and high Reynolds number data at the large values of X_c/D .

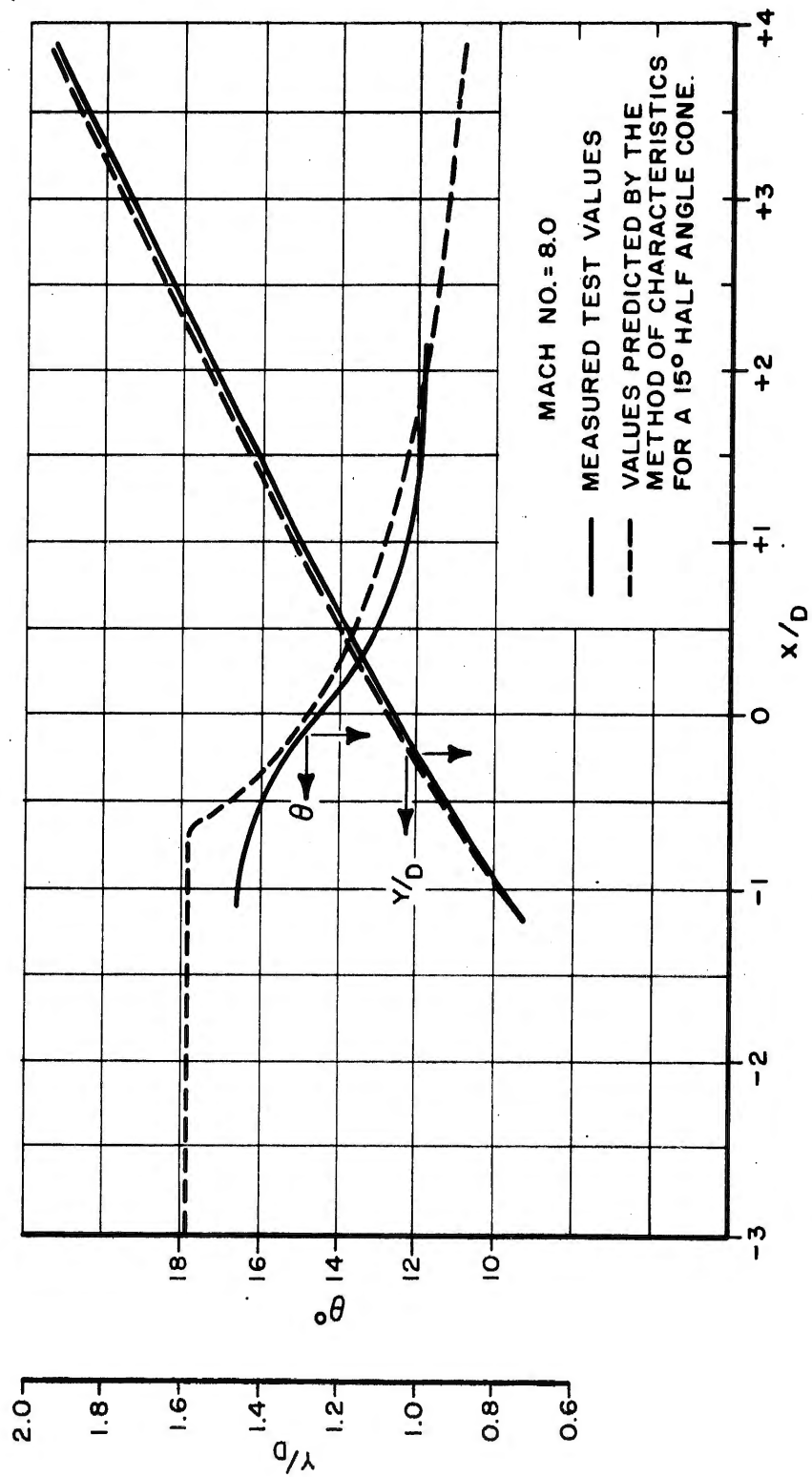


Figure 10 Comparison of Measured Shock Wave Location and Angle with Values Obtained from Characteristic Solution for a 15 degree Half Angle Cone, Cylinder Body Combination

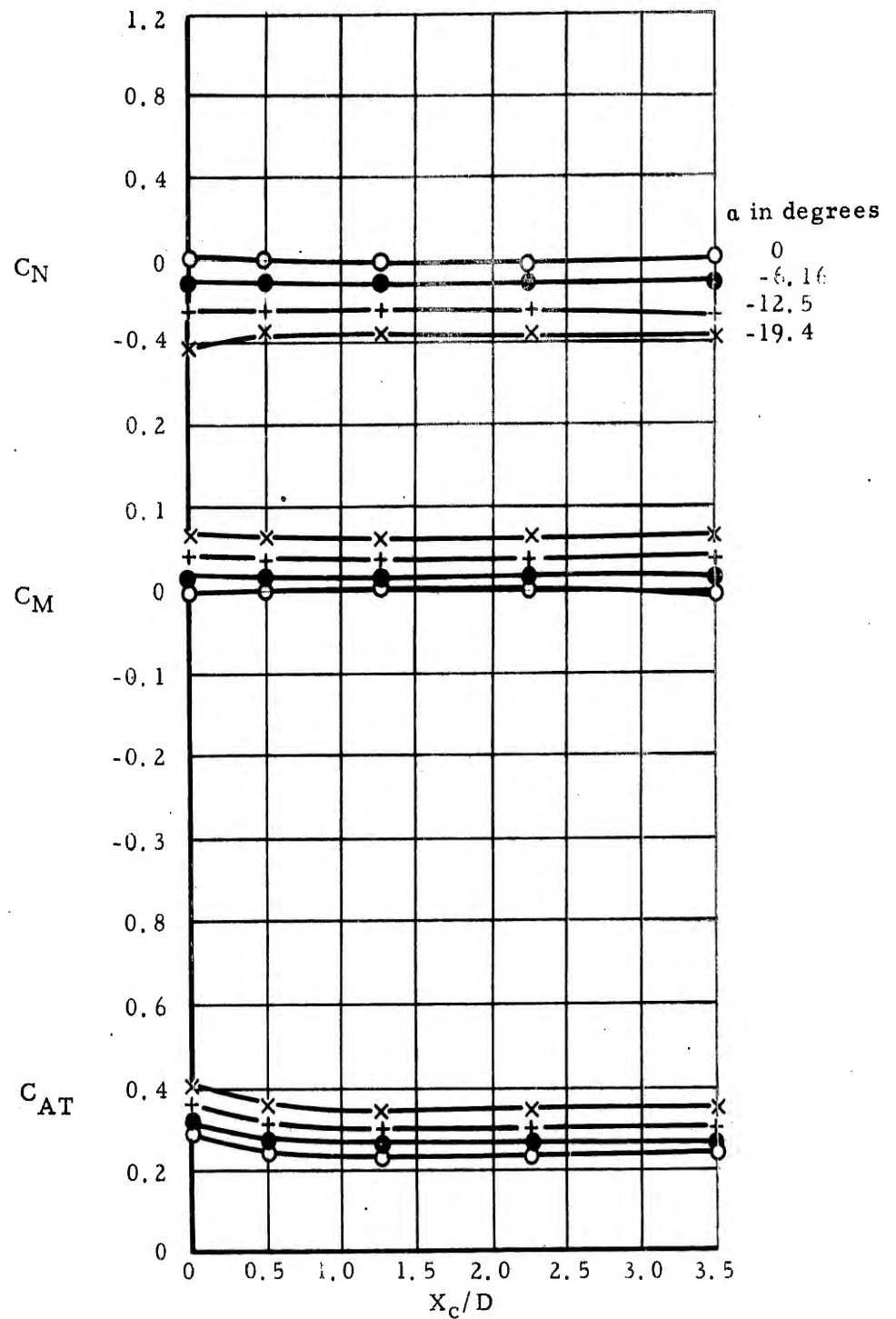


Figure 11a. Predicted Close-in Aerodynamic Coefficient - Variation of Capsule Characteristics with Axial Excursion in a Flow Field Generated by the Method of Characteristics for a 15 Degree Half Angle Cone Cylinder Lateral Station $Y_c/D = .75$

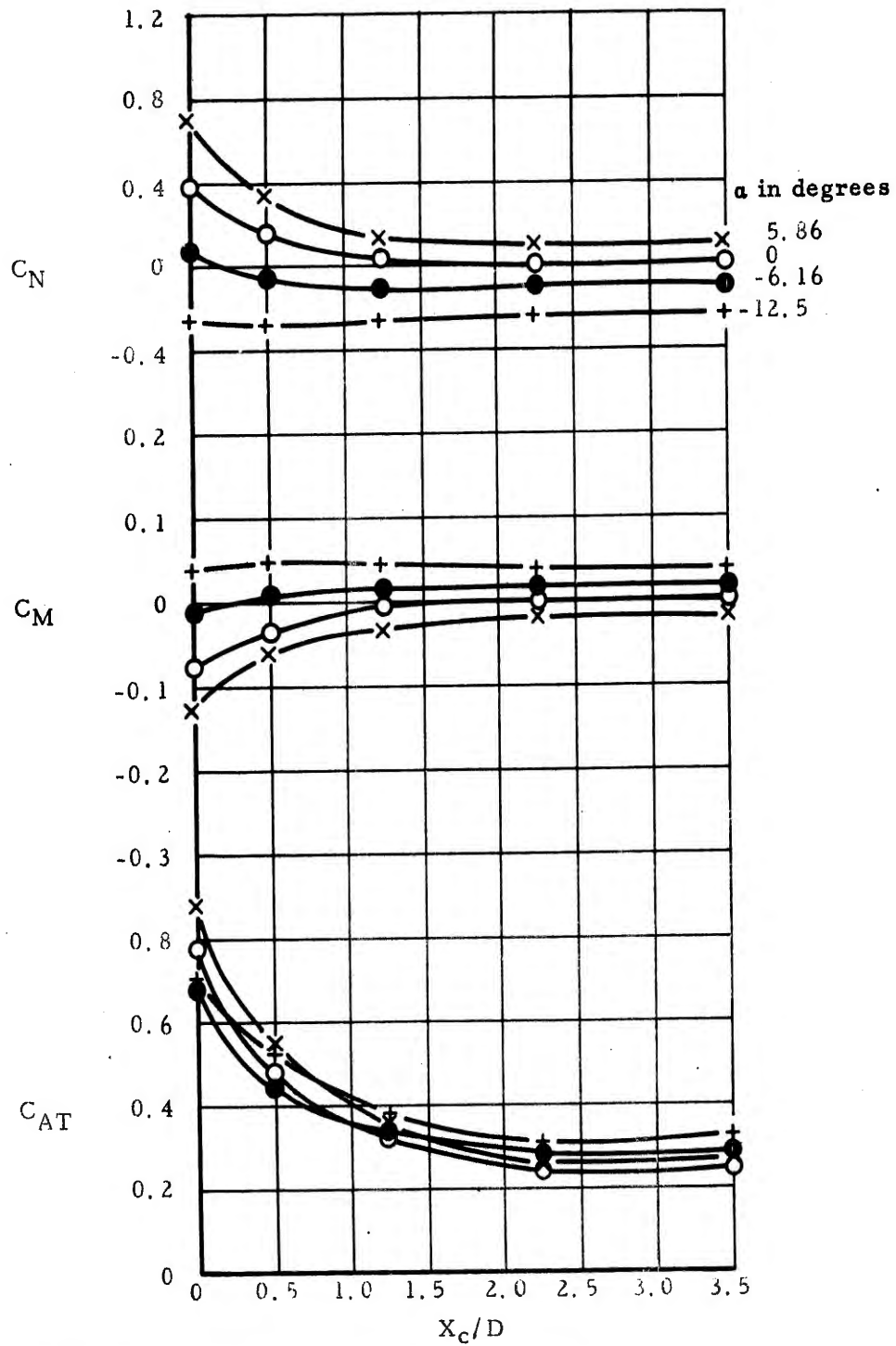


Figure 11b. Predicted Close-in Aerodynamic Coefficient - Variation of Capsule Characteristics with Axial Excursion in a Flow Field Generated by the Method of Characteristics for a 15 Degree Half Angle Cone Cylinder
Lateral Station $Y_c/D = 1.00$

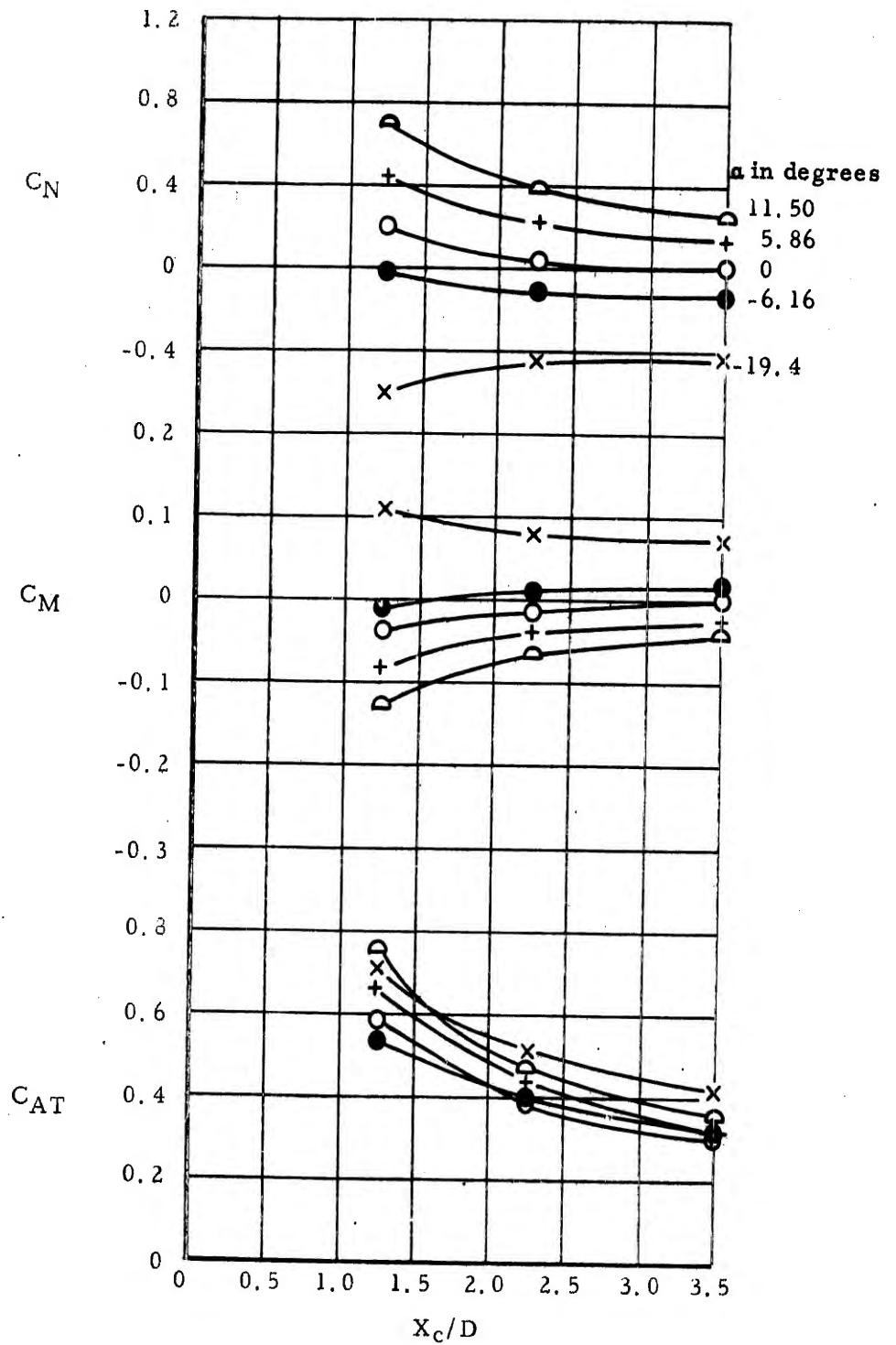


Figure 11c. Predicted Close-in Aerodynamic Coefficient - Variation of Capsule Characteristics with Axial Excursion in a Flow Field Generated by the Method of Characteristics for a 15 Degree Half Angle Cone Cylinder Lateral Station $Y_c/D = 1.25$

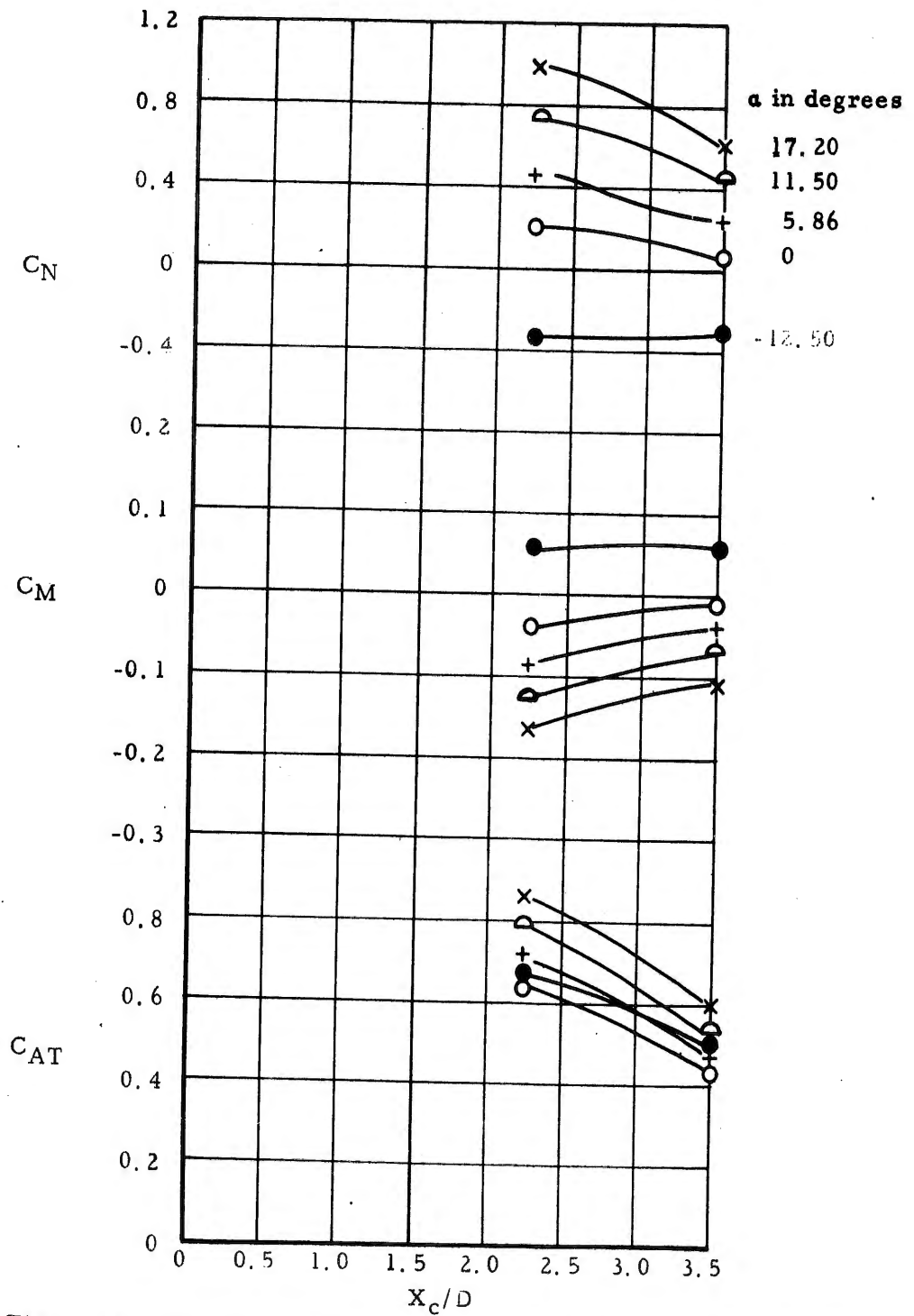


Figure 11d. Predicted Close-in Aerodynamic Coefficient - Variation of Capsule Characteristics with Axial Excursion in a Flow Field Generated by the Method of Characteristics for a 15 Degree Half Angle Cone Cylinder Lateral Station $Y_c/D = 1.50$

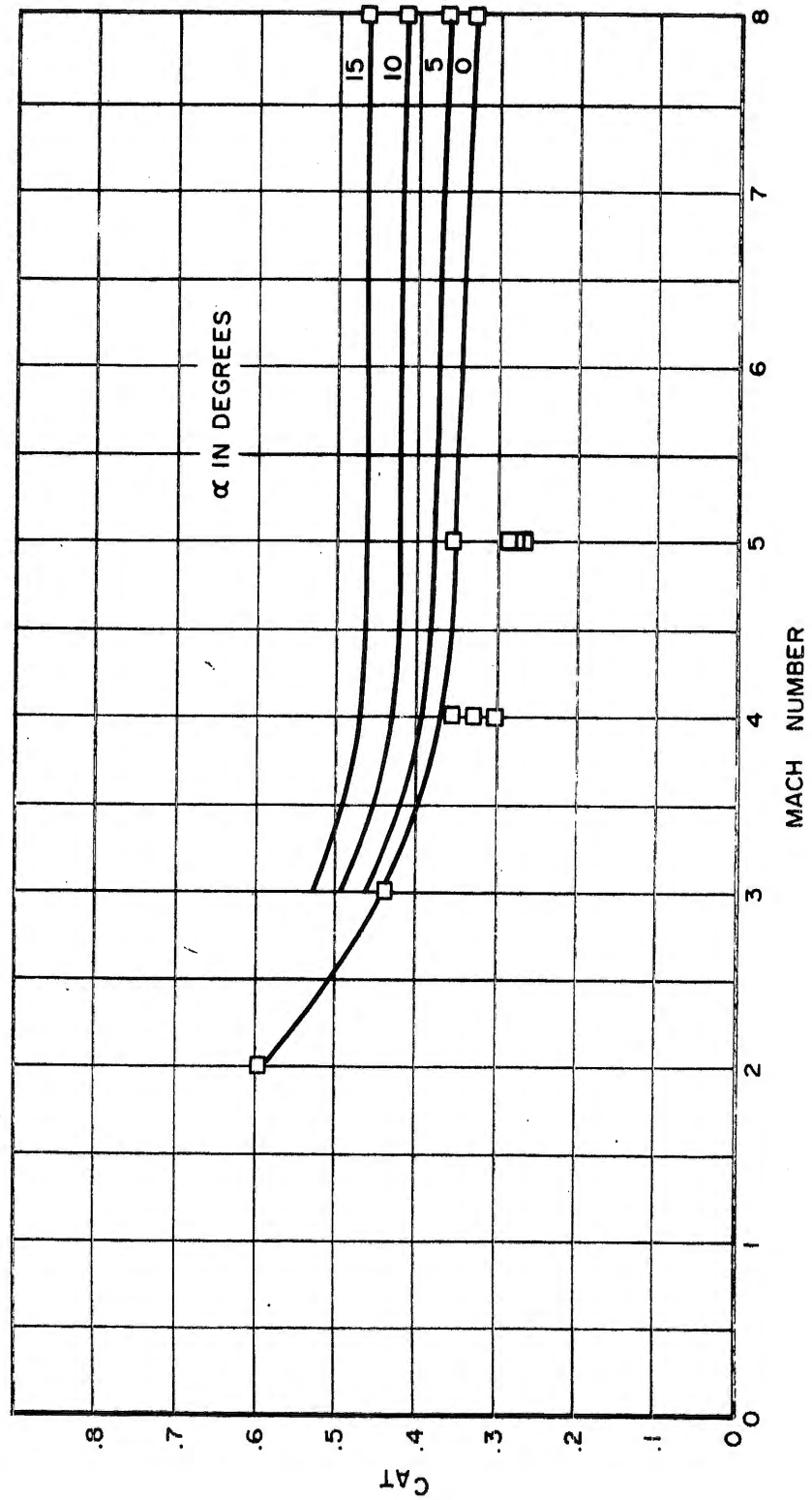


Figure 12. Capsule Axial Force Coefficient Variation with Free Stream Mach Number and Various Reynolds Numbers

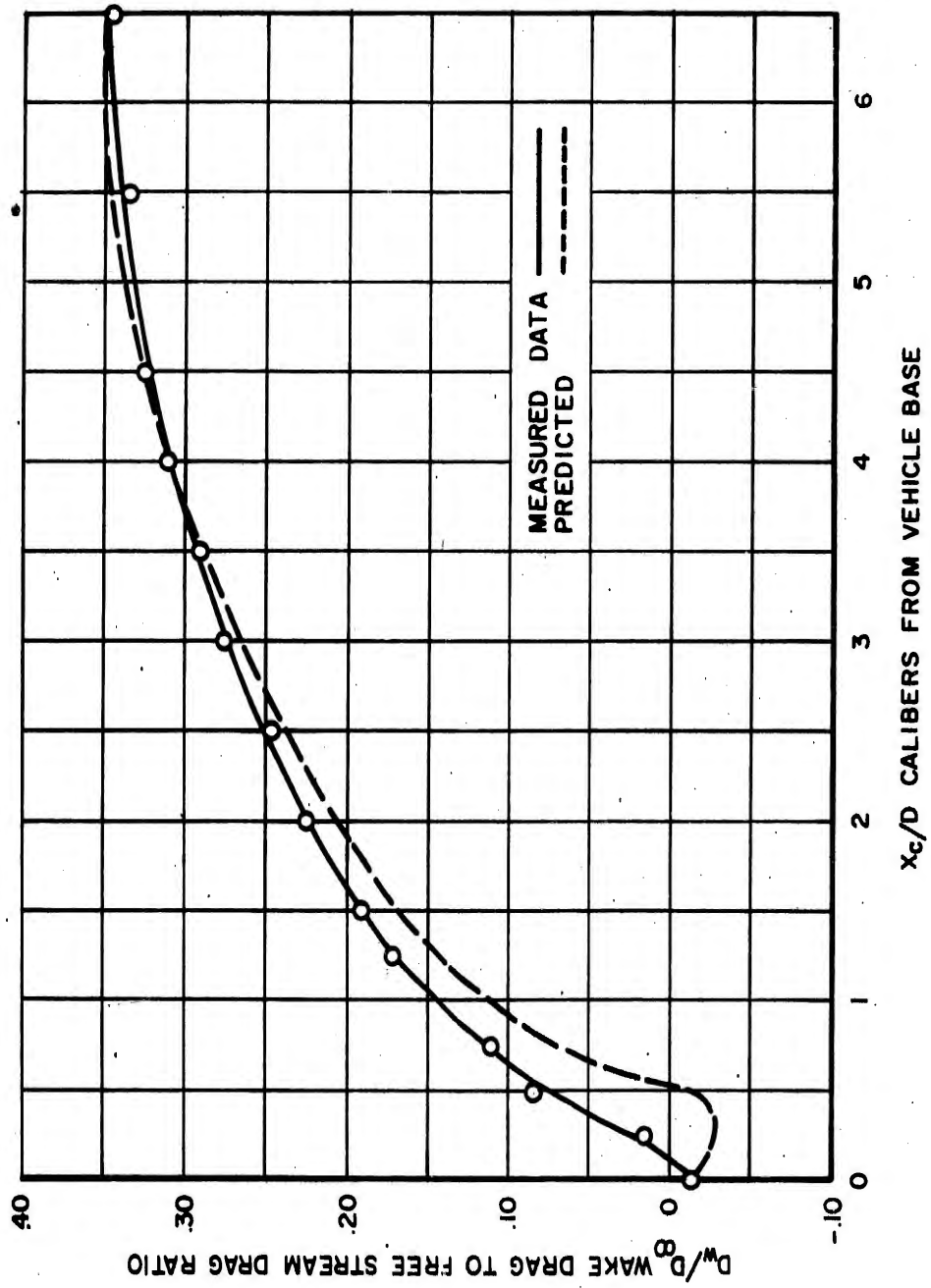


Figure 13a. Comparison of Predicted and Experimental Data for Wake Core Drag Ratio - $Re = 3.36 \times 10^6$ ft

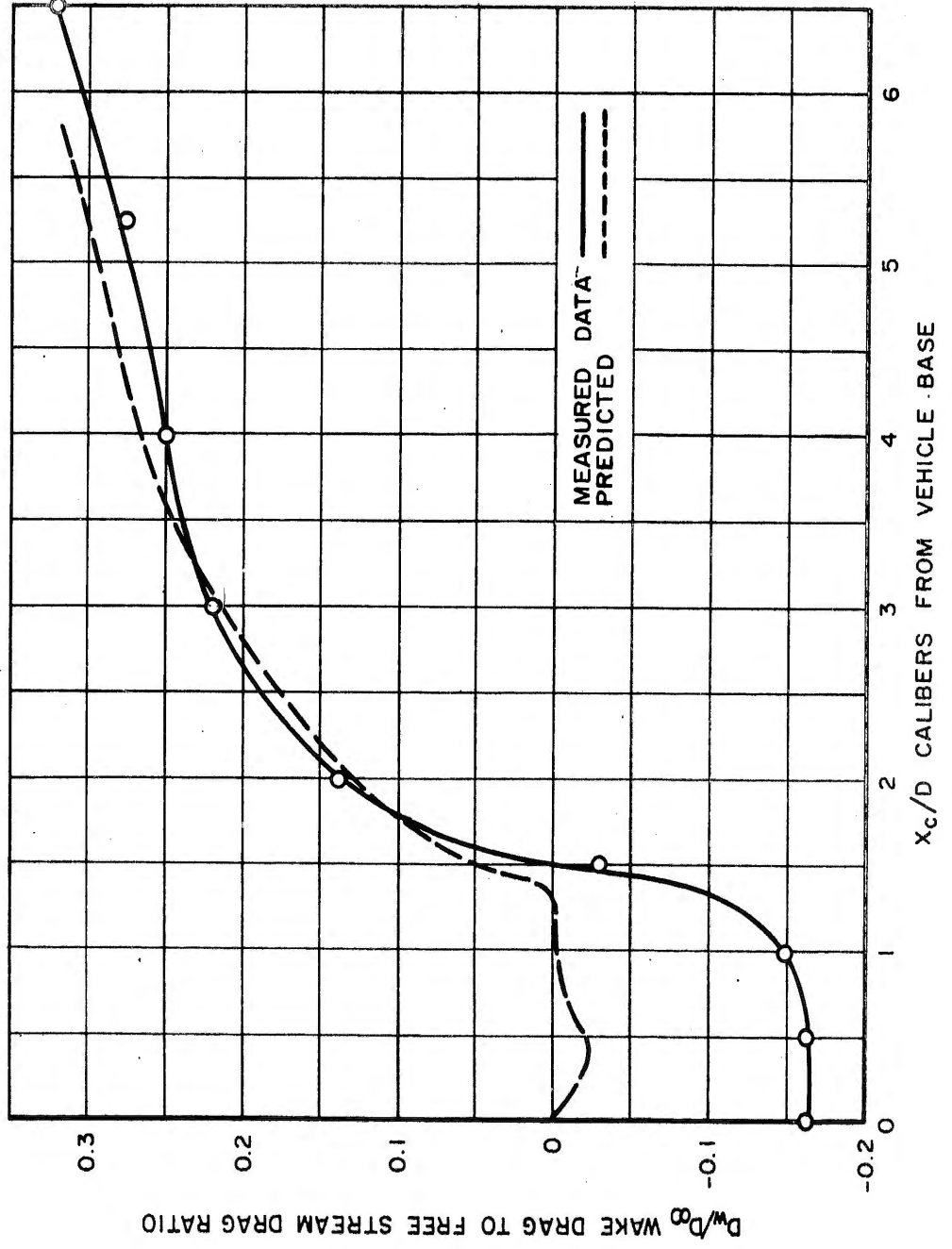


Figure 13b. Comparison of Predicted and Experimental Data
For Wake, Core Drag Ratio - $Re = 1.6 \times 10^6 / Ft.$

SECTION V

CONCLUSIONS

The comparison of the predicted and wind tunnel data described in Section III indicates that for most of the phases studied, reasonable agreement between the measured and predicted trends can be obtained by using free stream capsule characteristics and correcting these with the local Mach number, dynamic pressure ratio and flow field inclination angle. Analysis performed in this report has been limited to considering the capsule flow field parameters as those which prevail at the capsule's midpoint in an undisturbed flow field. It is believed, and results shown in Volume II substantiate, that using strip theory or some other type of analytical procedure such as that of Moskowitz (Ref. 4), which accounts for gradients in the flow field, would improve the accuracy of the predicted values. This improvement would be expected to be most pronounced in the close-in region where the capsule is close to or in the carrier shockwave, and in the wake penetration region where the capsule is in the expansion region at the vehicle base. Both of these regions produce large gradients in flow field characteristics and represent regions where the most significant disagreement has been encountered in the predicted and measured values.

Reasonable agreement between the predicted and measured axial force coefficients are obtained for the wake interaction region aft of the assumed wake minimum thickness location for the high Reynolds number tests. For the regions between the vehicle base and the minimum wake thickness at the high Reynolds number, accounting for the horizontal pressure buoyancy correction such as that shown by Love (Ref. 6), predictions reasonably indicate the trend in axial force decay. However, the curve is displaced (conservatively for ejection velocity requirements) by approximately 0.25 calibers. The results of these calculations for a Mach number of 8 and those performed in Volume II for a Mach number of 4, indicate that for Reynolds numbers equal to or above that for the Mach 8 tests ($Re_{\infty} = 3.36 \times 10^6$) reasonable estimates of the required ejection velocity for a capsule based on static data can be made for this Mach number range by using the prediction procedure described in Volume II. Dynamic test results will be required however, to determine the adequacy of using static measurements for free-flight models.

For the low Reynolds number test, it was not possible to use the predicted wake minimum thickness location as given by Love to obtain agreement with the data. These data indicate that for a tunnel Reynolds number of 1.69×10^6 per foot, a rearward shift in the minimum thickness location occurs. This shift (approximately 0.8 calibers) was estimated by fitting the prediction procedure used for the high Reynolds number data and working

backward to predict the wake throat location. The axial force measurements in the region forward of the wake throat was impossible to predict using the technique used for the high Reynolds number data. Additional test data are required before any reasonable prediction technique can be obtained for low Reynolds number data. It is also cautioned that for carrier and capsule Reynolds numbers in this range, these data indicate that a sizeable increase would be required in ejection velocities over that predicted by the above-described procedure to assure capsule separation.

As a result of the data obtained for Mach numbers of 2, 4, 5 and 8 reported in Volume II and this report, it is recommended that upon conclusion of the dynamic wind tunnel investigation which will be reported in Volume IV, trajectories be computed using predicted values obtained from the relatively simple procedure outlined in this report. This technique could then be compared to the measured dynamic trajectories and final determination of whether the inclusion of the additional refinements (which increase the complexity) are required to predict the capsule's over-all motion. The above recommendation is contingent however, on the premise that large deviations in static measurements are not found as a result of relative motion between the carrier and capsule.

REFERENCES

1. Wackelin, H., and Fredette, R., Dynamics of Separating Bodies, Volume II, "Measurements at Mach 2, 4, and 5" AFOSR-106
2. Kayser, L., and Merz, G., Force Measurements on a Data Capsule in the Wake and Flow Field of a Carrier Vehicle at Mach 8, AEDC-TDR-62-220
3. Mc Cauley, W. D., The Aerodynamic Design and Evaluation of a Second Generation ICBM Nose Cone, The General Electric Mark 3, Volume II, Entry Vehicles and Hypersonics, Transactions of the Fourth Symposium on Ballistic Missiles and Space Technology, 24-27 August 1959.
4. Moskowitz, B., Approximate Theory for Calculation of Lift of Bodies, Afterbodies, and Combinations of Bodies, NACA-TN-2418.
5. Solarski, A., Turner, R., and Doerr, F., Dynamics of Separating Bodies, Volume I, "Theoretical Analysis", AFOSR-109
6. Love, E., Base Pressure at Supersonic Speeds on Two-Dimensional Airfoils and on Bodies of Revolution with and without Fins having Turbulent Boundary Layers, NACA TN-3819
7. Coats, J. D., Static and Dynamic Testing of Conical Trailing Decelerators for the Pershing Re-Entry Vehicle, AEDC TN-60-188
8. Howarth, L., Editor, Modern Development in Fluid Dynamics, "High Speed Flow", Volume II, Oxford at the Clarendon Press, 1953

<p>Office of Research Analyses Office of Aerospace Research Holloman AFB, New Mexico 88330</p> <p>DYNAMICS OF SEPARATING BODIES - MEASUREMENTS AT MACH 8, Vol III, November 1963. 49pp incl illus. ORA-63-13 unclassified report</p> <p>Additional wind tunnel tests at a Mach number of 8, which supplemented Mach 2, 4, and 5 tests reported in Vol II, on a data capsule shape in an interference flow field of a carrier vehicle were conducted. The data obtained were (over)</p>	<p>UNCLASSIFIED</p> <p>1. Dynamics of Separation</p> <p>2. Wind Tunnel Tests, Supersonic</p> <p>3. Ejection - Capsules</p> <p>I. Contr AF29(600) 1711, Proj 7856 Task 78548 Cook Res. Lab. Chicago, Ill.</p> <p>III. R. D. Turner</p> <p>IV. In DDC Collection</p> <p>UNCLASSIFIED</p>	<p>Office of Research Analyses Office of Aerospace Research Holloman AFB, New Mexico 88330</p> <p>DYNAMICS OF SEPARATING BODIES - MEASUREMENTS AT MACH 8, Vol III, November 1963. 49pp incl illus. ORA-63-13 unclassified report</p> <p>Additional wind tunnel tests at a Mach number of 8, which supplemented Mach 2, 4, and 5 tests reported in Vol II, on a data capsule shape in an interference flow field of a carrier vehicle were conducted. The data obtained were (over)</p>	<p>UNCLASSIFIED</p> <p>1. Dynamics of Separation</p> <p>2. Wind Tunnel Tests, Supersonic</p> <p>3. Ejection - Capsules</p> <p>I. Contr AF29(600) 1711, Proj 7856 Task 78548 Cook Res. Lab. Chicago, Ill.</p> <p>III. R. D. Turner</p> <p>IV. In DDC Collection</p> <p>UNCLASSIFIED</p>
<p>Office of Research Analyses Office of Aerospace Research Holloman AFB, New Mexico 88330</p> <p>DYNAMICS OF SEPARATING BODIES - MEASUREMENTS AT MACH 8, Vol III, November 1963. 49pp incl illus. ORA-63-13 unclassified report</p> <p>Additional wind tunnel tests at a Mach number of 8, which supplemented Mach 2, 4, and 5 tests reported in Vol II, on a data capsule shape in an interference flow field of a carrier vehicle were conducted. The data obtained were (over)</p>	<p>UNCLASSIFIED</p> <p>1. Dynamics of Separation</p> <p>2. Wind Tunnel Tests, Supersonic</p> <p>3. Ejection - Capsules</p> <p>I. Contr AF29(600) 1711, Proj 7856 Task 78548 Cook Res. Lab. Chicago, Ill.</p> <p>III. R. D. Turner</p> <p>IV. In DDC Collection</p> <p>UNCLASSIFIED</p>	<p>Office of Research Analyses Office of Aerospace Research Holloman AFB, New Mexico 88330</p> <p>DYNAMICS OF SEPARATING BODIES - MEASUREMENTS AT MACH 8, Vol III, November 1963. 49pp incl illus. ORA-63-13 unclassified report</p> <p>Additional wind tunnel tests at a Mach number of 8, which supplemented Mach 2, 4, and 5 tests reported in Vol II, on a data capsule shape in an interference flow field of a carrier vehicle were conducted. The data obtained were (over)</p>	<p>UNCLASSIFIED</p> <p>1. Dynamics of Separation</p> <p>2. Wind Tunnel Tests, Supersonic</p> <p>3. Ejection - Capsules</p> <p>I. Contr AF29(600) 1711, Proj 7856 Task 78548 Cook Res. Lab. Chicago, Ill.</p> <p>III. R. D. Turner</p> <p>IV. In DDC Collection</p> <p>UNCLASSIFIED</p>

<p>analyzed and a preliminary evaluation was made to the agreement with methods of prediction for both the Mach 8 tests and previous reported tests. It is shown that where the interference flow field is reasonably predicted estimated values of a capsule's derivatives obtained with relatively simple calculation techniques agree reasonably well with the data.</p> <p style="text-align: center;">○</p>	<p>UNCLASSIFIED</p>	<p>analyzed and a preliminary evaluation was made to the agreement with methods of prediction for both the Mach 8 tests and previous reported tests. It is shown that where the interference flow field is reasonably predicted estimated values of a capsule's derivatives obtained with relatively simple calculation techniques agree reasonably well with the data.</p> <p style="text-align: center;">○</p>	<p>UNCLASSIFIED</p>
<p>analyzed and a preliminary evaluation was made to the agreement with methods of prediction for both the Mach 8 tests and previous reported tests. It is shown that where the interference flow field is reasonably predicted estimated values of a capsule's derivatives obtained with relatively simple calculation techniques agree reasonably well with the data.</p> <p style="text-align: center;">○</p>	<p>UNCLASSIFIED</p>	<p>analyzed and a preliminary evaluation was made to the agreement with methods of prediction for both the Mach 8 tests and previous reported tests. It is shown that where the interference flow field is reasonably predicted estimated values of a capsule's derivatives obtained with relatively simple calculation techniques agree reasonably well with the data.</p> <p style="text-align: center;">○</p>	<p>UNCLASSIFIED</p>

<p>Office of Research Analyses Office of Aerospace Research Holloman AFB, New Mexico 88330</p> <p>DYNAMICS OF SEPARATING BODIES - MEASUREMENTS AT MACH 8, Vol III, November 1963. 49pp incl illus. ORA-63-13 unclassified report</p> <p>Additional wind tunnel tests at a Mach number of 8, which supplemented Mach 2, 4, and 5 tests reported in Vol II, on a data capsule shape in an interference flow field of a carrier vehicle were conducted. The data obtained were (over)</p>	<p>UNCLASSIFIED</p> <ol style="list-style-type: none"> 1. Dynamics of Separation 2. Wind Tunnel Tests, Supersonic 3. Ejection - Capsules <ol style="list-style-type: none"> I. Contr AF29(600) 1711, Proj 7856 Task 78548 Cook Res. Lab. Chicago, Ill. II. In DDC Collection <p>UNCLASSIFIED</p>	<p>Office of Research Analyses Office of Aerospace Research Holloman AFB, New Mexico 88330</p> <p>DYNAMICS OF SEPARATING BODIES - MEASUREMENTS AT MACH 8, Vol III, November 1963. 49pp incl illus. ORA-63-13 unclassified report</p> <p>Additional wind tunnel tests at a Mach number of 8, which supplemented Mach 2, 4, and 5 tests reported in Vol II, on a data capsule shape in an interference flow field of a carrier vehicle were conducted. The data obtained were (over)</p>	<p>UNCLASSIFIED</p> <ol style="list-style-type: none"> 1. Dynamics of Separation 2. Wind Tunnel Tests, Supersonic 3. Ejection - Capsules <ol style="list-style-type: none"> I. 1711, Proj 7856 Contr AF29(600) Task 78548 Cook Res. Lab. Chicago, Ill. II. R. D. Turner In DDC Collection <p>UNCLASSIFIED</p>
<p>Office of Research Analyses Office of Aerospace Research Holloman AFB, New Mexico 88330</p> <p>DYNAMICS OF SEPARATING BODIES - MEASUREMENTS AT MACH 8, Vol III, November 1963. 49pp incl illus. ORA-63-13 unclassified report</p> <p>Additional wind tunnel tests at a Mach number of 8, which supplemented Mach 2, 4, and 5 tests reported in Vol II, on a data capsule shape in an interference flow field of a carrier vehicle were conducted. The data obtained were (over)</p>	<p>UNCLASSIFIED</p> <ol style="list-style-type: none"> 1. Dynamics of Separation 2. Wind Tunnel Tests, Supersonic 3. Ejection - Capsules <ol style="list-style-type: none"> I. Contr AF29(600) 1711, Proj 7856 Task 78548 Cook Res. Lab. Chicago, Ill. II. R. D. Turner In DDC Collection <p>UNCLASSIFIED</p>	<p>Office of Research Analyses Office of Aerospace Research Holloman AFB, New Mexico 88330</p> <p>DYNAMICS OF SEPARATING BODIES - MEASUREMENTS AT MACH 8, Vol III, November 1963. 49pp incl illus. ORA-63-13 unclassified report</p> <p>Additional wind tunnel tests at a Mach number of 8, which supplemented Mach 2, 4, and 5 tests reported in Vol II, on a data capsule shape in an interference flow field of a carrier vehicle were conducted. The data obtained were (over)</p>	<p>UNCLASSIFIED</p> <ol style="list-style-type: none"> 1. Dynamics of Separation 2. Wind Tunnel Tests, Supersonic 3. Ejection - Capsules <ol style="list-style-type: none"> I. Contr AF29(600) 1711, Proj 7856 Task 78548 Cook Res. Lab. Chicago, Ill. II. R. D. Turner In DDC Collection <p>UNCLASSIFIED</p>

<p>analyzed and a preliminary evaluation was made to the agreement with methods of prediction for both the Mach 8 tests and previous reported tests. It is shown that where the interference flow field is reasonably predicted estimated values of a capsule's derivatives obtained with relatively simple calculation techniques agree reasonably well with the data.</p> <p style="text-align: center;">○</p>	<p>UNCLASSIFIED</p>	<p>analyzed and a preliminary evaluation was made to the agreement with methods of prediction for both the Mach 8 tests and previous reported tests. It is shown that where the interference flow field is reasonably predicted estimated values of a capsule's derivatives obtained with relatively simple calculation techniques agree reasonably well with the data.</p> <p style="text-align: center;">○</p>	<p>UNCLASSIFIED</p>
<p>analyzed and a preliminary evaluation was made to the agreement with methods of prediction for both the Mach 8 tests and previous reported tests. It is shown that where the interference flow field is reasonably predicted estimated values of a capsule's derivatives obtained with relatively simple calculation techniques agree reasonably well with the data.</p> <p style="text-align: center;">○</p>	<p>UNCLASSIFIED</p>	<p>analyzed and a preliminary evaluation was made to the agreement with methods of prediction for both the Mach 8 tests and previous reported tests. It is shown that where the interference flow field is reasonably predicted estimated values of a capsule's derivatives obtained with relatively simple calculation techniques agree reasonably well with the data.</p> <p style="text-align: center;">○^e</p>	<p>UNCLASSIFIED</p>

UNCLASSIFIED

UNCLASSIFIED